ISOTROPIC TURBULENCE AND INERTIAL-RANGE STRUCTURE IN THE ABRIDGED LHDI APPROXIMATION

Robert H. Kraichnan

Peterborough, New Hampshire

Research Report No. 8

Task NR 062-309 Contract Nonr 4307(00)

January 1966

This work was supported by the Fluid Dynamics Branch of the Office of Naval Research under Contract Nonr 4307(00). Reproduction in whole or in part is permitted for any purpose of the United States Government. Distribution of this report is unlimited.

ISOTROPIC TURBULENCE AND INERTIAL-RANGE STRUCTURE IN THE ABRIDGED LHDI APPROXIMATION

Robert H. Kraichnan

Peterborough, New Hampshire

The abridged LHDI (Lagrangian-History Direct Interaction) closure approximation is interpreted physically and used to analyze energy transfer, effective eddy viscosities, and Lagrangian spacetime statistics in stationary and decaying isotropic turbulence. The results are then specialized to the inertial range. Numerical values are predicted for the Kolmogorov constant, the asymptotic eddy viscosities due to inertial-range wavenumbers, and the dimensionless constant in Inoue's formula for the mean square change of Lagrangian velocity with time. Computed curves are presented for the localness of energy transfer, for Lagrangian spacetime structure functions, and for Lagrangian spacetime acceleration-acceleration and velocity-acceleration covariances. Inertial-range Eulerian spacetime structure functions also are computed. The predicted absolute Kolmogorov spectrum in the inertial and dissipation ranges is compared with data of Grant, Stewart, and Moilliet and of M. M. Gibson.

ACKNOWLEDGMENTS

This work was supported by the Fluid Dynamics Branch of the Office of Naval Research under Contract Nonr 4307(00). The machine computations were performed through the courtesy of the Goddard Institute of Space Studies. Mr. Randy Rustin and Mr. George Kleiner assisted with the computations.

1. INTRODUCTION

This paper develops some analytical and numerical predictions of recent closure approximations which involve tracing the history of velocity correlations along the particle trajectories.[1] Energy transfer, and both Lagrangian and Eulerian spacetime correlations are explored for stationary and decaying isotropic turbulence. Simple physical interpretations of the closure formulas and their consequences are attempted. The results are finally specialized to the inertial range, and numerical values are computed for all the dimensionless constants and universal functions which appear in the formulas. The quantities evaluated are listed in the abstract. Analytical and numerical predictions for two-particle dispersion are developed in a paper to follow.

The closure approximations of Ref. 1 are based on a generalized velocity $\underset{\sim}{u}(\underset{\sim}{x},t|r)$, defined as the velocity measured at time r in that fluid element which arrives at $\underset{\sim}{x}$, in laboratory coordinates, at time t. Thus,

$$\underset{\sim}{u}(\underset{\sim}{x},t|t) = \underset{\sim}{u}(\underset{\sim}{x},t), \tag{1.1}$$

where $\underset{\sim}{u}(\underset{\sim}{x},t)$ is the Eulerian velocity, and $\underset{\sim}{u}(\underset{\sim}{a},t_0|t) = \underset{\sim}{w}(\underset{\sim}{a},t)$, where t_0 is the initial time and $\underset{\sim}{w}(\underset{\sim}{a},t)$ is the velocity of the particle initially at $\underset{\sim}{a}$ (Lagrangian velocity).

The full function $\underset{\sim}{u}(\underset{\sim}{x},t|r)$ can be computed in terms of the Eulerian velocity by the equation[1]

$$[\partial/\partial t + \underset{\sim}{u}(\underset{\sim}{x},t)\cdot\underset{\sim}{\nabla}]\underset{\sim}{u}(\underset{\sim}{x},t|r) = 0, \tag{1.2}$$

with the boundary condition (1.1). The interpretation of (1.2) is simple.

The vector $\underset{\sim}{u}(\underset{\sim}{x},t|r)$ is the velocity of a particular fluid element at time r, and $(\underset{\sim}{x},t)$ is a point on the spacetime trajectory of this element. Thus t may be called the labeling time and r, the measuring time. The same fluid element can be labeled by any other point $(\underset{\sim}{x}',t')$ on its trajectory, and the velocity measured at time r is independent of which point is used for labeling. Equation (1.2) expresses this by stating that the substantial derivative of $\underset{\sim}{u}(\underset{\sim}{x},t|r)$ in the spacetime $(\underset{\sim}{x},t)$ vanishes everywhere. In other words, $\underset{\sim}{u}(\underset{\sim}{x},t|r)$ at fixed r is constant along every particle trajectory in $(\underset{\sim}{x},t)$ spacetime.

Equation (1.2) thus has a peculiar character. It expresses only a coordinate transformation through which the velocity field at time r is labeled by the laboratory coordinates the fluid elements had (or will have) at time t. The dynamics are fully determined by the equation of motion for the Eulerian velocity $\underset{\sim}{u}(\underset{\sim}{x},t)$. The role of (1.2) is to provide a redundant, but useful, infinite family of transformed representations of the Eulerian field. Such a family is useful because approximate statistical equations are the ultimate goal. Although the Lagrangian velocity is fully determined by the Eulerian velocity in any realization, simple statistics of the Lagrangian velocity are not determined by simple statistics of the Eulerian velocity.

No restriction to incompressibility is implied by (1.2), which is valid whatever the equation of motion for $\underset{\sim}{u}(\underset{\sim}{x},t)$. The latter will be the incompressible Navier-Stokes equation in this paper.

Because the labeling transformation as well as the dynamics determine $\underset{\sim}{u}(\underset{\sim}{x},t|r)$, the generalized velocity has properties that are unexpected from

experience with Eulerian analysis. It was pointed out in Ref. 1 that divergenceless Eulerian velocity does not imply divergenceless $\underset{\sim}{u}(\underset{\sim}{x},t|r)$ for $r \neq t$. To explore another property, consider a hypothetical flow maintained in a statistically steady and isotropic state at very low Reynolds number by means of suitably random stirring devices. If D is a characteristic length scale of the stirring process, the characteristic scale of spatial variation of the Eulerian field $\underset{\sim}{u}(\underset{\sim}{x},t)$ will also be D, and the condition of very low Reynolds number implies that variations at scales small compared to D will be strongly damped. If a Fourier analysis of $\underset{\sim}{u}(\underset{\sim}{x},t)$ is made, wavenumbers $>>D^{-1}$ should be very weakly excited.

Now consider $\underset{\sim}{u}(\underset{\sim}{x},t|r)$ for large values of $|t-r|$. Although both $\underset{\sim}{u}(\underset{\sim}{x},t)$ and $\underset{\sim}{u}(\underset{\sim}{x},r)$ display spatial variation at scale D, the $\underset{\sim}{x}$ variation of $\underset{\sim}{u}(\underset{\sim}{x},t|r)$ becomes rapid without limit as $|t-r|$ increases. This is because fluid elements which are close together at the labeling time t will typically be farther apart at time r. No matter how small $|\underset{\sim}{x}-\underset{\sim}{x}'|$ is taken, $\underset{\sim}{u}(\underset{\sim}{x},t|r)$ and $\underset{\sim}{u}(\underset{\sim}{x}',t|r)$ typically are velocities measured at widely separated parts of the fluid if $|t-r|$ is large enough. For sufficiently large $|t-r|$, the Fourier analysis of $\underset{\sim}{u}(\underset{\sim}{x},t|r)$ shows excitation extending to indefinitely high wavenumbers. In particular, the excitation does not fall off at the viscous cutoff wavenumber for the Eulerian velocity.

The assumption of low Reynolds number puts these observations in their most striking form but is otherwise unnecessary. To examine a further property, retain the stationarity, isotropy, and homogeneity conditions but relax the restriction to small Reynolds number. The Eulerian covariance $\langle \underset{\sim}{u}(\underset{\sim}{x},t)\cdot\underset{\sim}{u}(\underset{\sim}{x}',r)\rangle$, where $\langle\ \rangle$ denotes ensemble average, is an even function

of t-r and has zero slope at r = t. This is not true of the Lagrangian covariance $\langle \underset{\sim}{u}(\underset{\sim}{x},t|t)\cdot\underset{\sim}{u}(\underset{\sim}{x}',t|r)\rangle$, unless $\underset{\sim}{x}' = \underset{\sim}{x}$. The behavior of the Lagrangian covariance can be understood as follows. Two fluid elements which are a distance $|\underset{\sim}{x}-\underset{\sim}{x}'|$ apart at time t were typically a greater distance apart at any sufficiently earlier time r. As the elements draw together under the straining action of the turbulence, the joint effects of molecular and eddy viscosity on the steepening velocity gradient between the elements tends to reduce their velocity difference, while the stirring action tends typically to increase the difference. If $|\underset{\sim}{x}-\underset{\sim}{x}'|$ is intermediate between the scale characteristic of the stirring and the scale characteristic of dissipation, the effect of the stirring on relative velocity is suppressed compared to the effect of molecular and eddy viscosity. The typical net result is a reduction of the velocity difference. As the elements again separate, their velocities tend to be better correlated than before the close approach. This suggests that the Lagrangian covariance is an asymmetrical function of r - t, for $\underset{\sim}{x} \neq \underset{\sim}{x}'$, and can have a positive slope at r = t. However, if $\underset{\sim}{x} = \underset{\sim}{x}'$, the covariance measures the autocorrelation of the velocity of a single fluid element, whence stationarity and the equivalence of all elements require that the covariance be an even function of r-t.

These properties are demonstrated analytically later in the paper. The slope at r = t is shown to be simply related to the energy-transfer function. In the limit of very low Reynolds number, transfer is negligible, stirring and viscosity act on the same spatial scale, and the slope tends to zero.

2. THE CLOSURE EQUATIONS

In isotropic, homogeneous turbulence, the covariance tensor

$$U_{ij}(\underset{\sim}{x},t|r;\underset{\sim}{x}',t'|r') = \left\langle u_i(\underset{\sim}{x},t|r)u_j(\underset{\sim}{x}',t'|r')\right\rangle \tag{2.1}$$

is fully determined by the scalars

$$U^S(\underset{\sim}{k};t|r;t'|r') = (2\pi)^{-3}\int e^{-i\underset{\sim}{k}\cdot(\underset{\sim}{x}-\underset{\sim}{x}')}P_{ij}(\underset{\sim}{k})U_{ij}(\underset{\sim}{x},t|r;\underset{\sim}{x}',t'|r')d(\underset{\sim}{x}-\underset{\sim}{x}'),$$

$$U^C(\underset{\sim}{k};t|r;t'|r') = (2\pi)^{-3}\int e^{-i\underset{\sim}{k}\cdot(\underset{\sim}{x}-\underset{\sim}{x}')}\Pi_{ij}(\underset{\sim}{k})U_{ij}(\underset{\sim}{x},t|r;\underset{\sim}{x}',t'|r')d(\underset{\sim}{x}-\underset{\sim}{x}'), \tag{2.2}$$

where

$$\Pi_{ij}(\underset{\sim}{k}) = k_ik_j/k^2, \quad P_{ij}(\underset{\sim}{k}) = \delta_{ij} - k_ik_j/k^2.$$

U^S and U^C are the scalars of the solenoidal and antisolenoidal parts of U_{ij}, respectively. $U^C(\underset{\sim}{k};t|r;t'|r')$ vanishes if either $t = r$ or $t' = r'$.

The closure approximations of Ref. 1 involve both the covariance tensor and a generalized infinitesimal Green's tensor $G_{ij}(\underset{\sim}{x},t|r;\underset{\sim}{x}',t'|r')$, which gives the average change in $\underset{\sim}{u}(\underset{\sim}{x},t|r)$ resulting from an applied infinitesimal perturbation in $\underset{\sim}{u}(\underset{\sim}{x}',t'|r')$. The definition and properties of the Green's tensor are discussed in detail in Ref. 1. The isotropic Green's tensor is fully determined by the scalars

$$G^S(\underset{\sim}{k};t|r;t'|r') = \frac{1}{2}\int e^{-i\underset{\sim}{k}\cdot(\underset{\sim}{x}-\underset{\sim}{x}')}P_{ij}(\underset{\sim}{k})G_{ij}(\underset{\sim}{x},t|r;\underset{\sim}{x}',t'|r')d(\underset{\sim}{x}-\underset{\sim}{x}'),$$

$$G^C(\underset{\sim}{k};t|r;t'|r') = \int e^{-i\underset{\sim}{k}\cdot(\underset{\sim}{x}-\underset{\sim}{x}')}\Pi_{ij}(\underset{\sim}{k})G_{ij}(\underset{\sim}{x},t|r;\underset{\sim}{x}',t'|r')d(\underset{\sim}{x}-\underset{\sim}{x}'). \tag{2.3}$$

$G^S(\underset{\sim}{k};t|r;t'|r')$ and $G^C(\underset{\sim}{k};t|r;t'|r')$ may be interpreted as average infinitesimal response functions for Fourier mode $\underset{\sim}{k}$. By definition,

$$G^S(\underset{\sim}{k};t|r;t|r) = G^C(\underset{\sim}{k};t|r;t|r) = 1,$$

$$G^S(\underset{\sim}{k};t|r;t'|r') = G^C(\underset{\sim}{k};t|r;t'|r') = 0 \qquad (r < r'). \tag{2.4}$$

Two closure approximations were proposed in Ref. 1. The first, called the LHDI (Lagrangian-History Direct-Interaction) approximation, involves all the time-argument values of the covariance and Green's functions. A closed subset of the final equations involves only functions for which $t = t'$. This approximation makes formidable storage and time demands in numerical computations. The second, simpler closure, called the abridged LHDI approximation, involves only the solenoidal, pure Lagrangian functions $U(k;t|r)$ and $G(k;t|r)$ defined by

$$\begin{aligned} U(k;t|r) &= U^S(\underset{\sim}{k};t|t;t|r) \qquad (t \geq r) \\ &= U(k;r|t) \qquad (t < r), \\ G(k;t|r) &= G^S(\underset{\sim}{k};t|t;t|r). \end{aligned} \tag{2.5}$$

The LHDI approximation was obtained in two stages. First, the direct-interaction approximations for triple moments were constructed. Then, the formulas were altered in a systematic way so that the final equations exhibited the following properties of the exact turbulence dynamics: Energy conservation; inviscid equipartition equilibrium and fluctuation-relaxation relations; invariance of Lagrangian correlations under random Galilean transformation; and invariance of certain averages under the transformation from Eulerian to Lagrangian coordinates. The crucial property in this list is invariance to random Galilean transformation. This invariance, not retained by the unaltered direct-interaction approximation, is a formal statement of the obvious fact that random, uniform

translations of the individual flows in a homogeneous ensemble cannot affect the mean energy-transfer. The LHDI approximation appears to be the unique alteration, within the general direct-interaction framework, which restores this invariance for the full Lagrangian covariance tensor without sacrificing the other properties listed. No cutoffs, parameters, or arbitrary functions are invoked. The motivations of the LHDI approximation, and the details of the alterations, are described at length in Secs. 1 and 6 of Ref. 1.

The abridged closure was obtained in Ref. 1 as a further approximation to the LHDI equations. It appears to be the unique alteration of the direct-interaction equations which gives a closed set of equations for the restricted quantities (2.5) and exhibits the consistency properties listed above. Thus the abridged LHDI equations may be considered a closure in their own right, rather than an approximation to an approximation.

Both closures assume that the velocity field is multivariate normal at an initial instant t_0. In the limit of very small Reynolds number, both closures yield triple-moment formulas which are indistinguishable from the first term in an expansion of the triple moments in powers of turbulent Reynolds number.[1]

The analysis in the present paper is based on the abridged LHDI equations, with the exception of the discussion of Eulerian structure-functions in Sec. 7. Quantitative estimates of how the numerical predictions change in the unabridged approximation have not been attempted. Qualitative changes in the predictions are not anticipated.

In the case of isotropic turbulence, the abridged equations of Ref. 1,

Sec. 10 may be written

$$(\partial/\partial t + 2\nu k^2)U(k;t|t) =$$

$$2\iint_\Delta dpdqB_{kpq}\int_{t_0}^{t}[G(k;t|s)U(p;t|s) - G(p;t|s)U(k;t|s)]U(q;t|s)ds, \quad (2.6)$$

$$(\partial/\partial t + \nu k^2)U(k;t|r) =$$

$$-U(k;t|r)\iint_\Delta dpdqC_{kpq}\int_r^t U(q;t|s)ds + \iint_\Delta dpdqD_{kpq}U(p;t|r)\int_r^t U(q;t|s)ds$$

$$+ \iint_\Delta dpdq\int_{t_0}^{r}[B_{kpq}G(k;r|s)U(p;t|s) - D'_{kpq}G(p;r|s)U(k;t|s)]U(q;t|s)ds$$

$$- \iint_\Delta dpdq\int_{t_0}^{t} B_{kpq}[G(p;t|s)U(k;r|s) - D_{kpq}G(k;t|s)U(p;r|s)]U(q;t|s)ds$$

$$- \iint_\Delta dpdq\int_{t_0}^{t}[B_{kpq} - D'_{kpq}]G(p;t|s)U(k;t|s)U(q;r|s)ds \quad (t \geq r), \quad (2.7)$$

$$(\partial/\partial t + \nu k^2)G(k;t|r) =$$

$$- G(k;t|r)\iint_\Delta dpdqC_{kpq}\int_r^t U(q;t|s)ds + \iint_\Delta dpdqD_{kpq}G(p;t|r)\int_r^t U(q;t|s)ds$$

$$- \iint_\Delta dpdq[D_{kpq} - B_{kpq}]G(p;t|r)U(q;t|r)\int_r^t G(k;s|r)ds$$

$$- \iint_\Delta dpdq\int_r^t [B_{kpq}G(p;t|s)G(k;s|r) - D'_{kpq}G(k;t|s)G(p;s|r)]U(q;t|s)ds$$

$$(t \geq r), \qquad G(k;r|r) = 1. \quad (2.8)$$

Here ν is kinematic viscosity, the integration $\iint_\Delta$ is over the part of the (p,q) plane such that k, p, q can form the sides of a triangle, and

$$B_{kpq} = \pi p^2 q(xy + z^3), \qquad C_{kpq} = \pi kpq(1 - y^2),$$

$$D_{kpq} = \frac{1}{2}(B_{kpq} + B_{kqp}) + \frac{1}{2}\pi kpq(z^2 - y^2), \quad D'_{kpq} = (p/k)^2 D_{pkq}, \tag{2.9}$$

where x, y, z are the cosines of the interior angles opposite the triangle sides k, p, q, respectively.[2] These equations, with (2.5), determine $U(k;t|r)$ and $G(k;t|r)$ for all $t \geq r \geq t_0$ if the initial values $U(k;t_0|t_0)$ are prescribed. The interpretation of (2.6)-(2.8) will be developed in the Sections to follow.

3. ENERGY TRANSFER

The kinetic-energy spectrum function

$$E(k,t) = 2\pi k^2 U(k;t|t) \tag{3.1}$$

obeys the balance equation

$$(\partial/\partial t + 2\nu k^2)E(k,t) = T(k,t), \tag{3.2}$$

where $T(k,t)/(2\pi k^2)$ is the right-hand side of (2.6). Conservation of energy,

$$\int_0^\infty T(k,t)dk = 0, \tag{3.3}$$

follows from the identity

$$k^2 B_{kpq} = p^2 B_{pkq}. \tag{3.4}$$

T(k,t) can be written in the form

$$T(k,t) = \frac{1}{2}\int_0^\infty dp \int_{|p-k|}^{p+k} dq\, T(k,p,q,t), \tag{3.5}$$

where $T(k,p,q,t)/(4\pi k^2)$ is the symmetrical part of the integrand of the p,q integration in (2.6). [The Δ integration, although written asymmetrically in (3.5), is symmetric in p and q so that only the symmetrical part of the integrand can contribute.] The detailed conservation property of the Navier-Stokes equation,

$$T(k,p,q,t) + T(p,q,k,t) + T(q,k,p,t) = 0, \tag{3.6}$$

follows from (3.4).

The total rate of energy transfer into all wavenumbers >k is

$$\Pi(k,t) = \frac{1}{2}\int_k^\infty dk' \int_0^\infty dp' \int_{|p'-k'|}^{p'+k'} dq' T(k',p',q',t). \tag{3.7}$$

Since $T(k',p',q',t)$ is symmetrical in p' and q', the total value of (3.7) must equal twice the contribution from q' > p'. But for q' > p' there is no net contribution for p' > k because, by (3.6), the interaction of k', p', q' then yields conservative transfer of energy within a triad of three wavenumbers all >k. Therefore (3.7) can be rewritten

$$\Pi(k,t) = \int_k^\infty dk' \int_0^k dp' \int_{p'_*}^{p'+k'} dq' T(k',p',q',t), \qquad (p'_* = \text{larger of } p',\ |p'-k'|). \tag{3.8}$$

This form is the more useful one for computing $\Pi(k,t)$. Since k' is always >k and p' always <k in (3.8), contributions from very small or very large wavenumbers always involve triads with a big ratio of largest to smallest wavenumber. If the transfer is effectively local in wavenumber, the integrations in (3.8) converge at zero and infinity in such fashion that only inertial-range k', p', q' contribute if k lies within a long inertial range. Equation (3.7), on the other hand, gives a nonlocal representation of $\Pi(k,t)$,

and a correct result is obtained from it for inertial-range k only if the integrations are extended to include the entire dissipation range.

Insight about the structure of the nonlinear interaction is provided by considering in detail the contributions to T(k,t) from interactions involving wavenumbers very much larger or very much smaller than k. Heisenberg[3] proposed that the effect of higher wavenumbers on T(k,t) could be represented by an eddy viscosity. The present closure approximation supports this hypothesis for wavenumbers much larger than k and yields an analytical expression for the eddy viscosity (different in form from Heisenberg's).

A Lagrangian time-correlation function for mode k can be defined by

$$R(k;t|r) = U(k;t|r)/[U(k;t|t)U(k;r|r)]^{1/2}. \tag{3.9}$$

To evaluate the asymptotic eddy viscosity, assume first that both E(k,t) and the characteristic decay times t-r of G(k;t|r) and R(k;t|r) decrease as k rises. If these conditions are satisfied with sufficient strength (to be checked later), the first term on the right-hand side of (2.6) gives a negligible part of the contribution to T(k,t) from wavenumbers >>k. The reason is that p >> k implies q >> k, and then U(k;t|s)U(q;t|s) >> U(p;t|s)U(q;t|s). Furthermore, U(k;t|s) ≈ U(k;t|t) in the second term, for s which make appreciable contributions. There results

$$T_{>q'}(k,t) = -2E(k,t)\int_{q'}^{\infty} dq \int_{q-k}^{q+k} dp B_{kpq} \int_{t_0}^{t} G(p;t|s)U(q;t|s)ds \tag{3.10}$$

for the contribution to T(k,t) from all q > q' >> k.

The integration in (3.10) is symmetric in p and q, to leading order in k/q. To leading order in k/q,

$$\frac{1}{2}(B_{kpq} - B_{kqp}) \approx -\pi q^3(u - u^3), \tag{3.11}$$

where u = (p-q)/k. The trigonometric identity

$$2A_{kpq} \equiv B_{kpq} + B_{kqp} = \pi kpq(1 - xyz - 2y^2z^2) \tag{3.12}$$

yields that to leading order

$$\frac{1}{2}(B_{kpq} + B_{kqp}) \approx \frac{1}{2}\pi kq^2(1 + u^2 - 2u^4). \tag{3.13}$$

If the G and U factors in (3.10) are expanded in Taylor series about u = 0, these expressions lead to

$$T_{>q}(k,t) = -2\nu_q(t)k^2E(k,t) \qquad (q >> k), \tag{3.14}$$

where

$$\nu_q(t) = \frac{2\pi}{15}\int_q^\infty [7\int_{t_0}^t G(p;t|s)U(p;t|s)ds - p\Delta(p,t)]p^2dp \tag{3.15}$$

and

$$\Delta(q,t) = \{\frac{\partial}{\partial p}\int_{t_0}^t [G(p;t|s)U(q;t|s) - G(q;t|s)U(p;t|s)]ds\}_{p=q}. \tag{3.16}$$

Note that the eddy viscosity $\nu_q(t)$ is independent of k and therefore is a true counterpart of molecular viscosity.

Now define $T_{<q}(k,t)$ as the total contribution to T(k,t) due to all interactions involving a wavenumber less than q. According to (3.14), the loss from wavenumber k due to interaction with much higher wavenumbers is proportional to the mean-square shear or vorticity associated with k. The interactions are conservative. Therefore $T_{<q}(k,t)$ should contain a contribution that involves $\nu_k(t)$ and the mean-square vorticity in wavenumbers

less than q, if q << k. Actually, the complete expression for $T_{<q}(k,t)$ cannot be deduced from $\nu_k(t)$ because the interaction is among triads rather than pairs of wavenumbers. The eddy viscosity represents the net loss of energy from low to pairs of high wavenumbers. In addition, the interaction with a low wavenumber induces a transfer of energy between the two high wavenumbers, and these two effects turn out to be of comparable importance in the overall energy transfer at the high wavenumbers.

The complete asymptotic expression for $T_{<q}(k,t)$ is

$$T_{<q'}(k,t) = 2k^2\int_0^{q'} E(q,t)q^{-2}dq\int_{k-q}^{k+q} dp\int_{t_0}^{t} [2A_{kpq}G(k;t|s)U(p;t|s) - B_{kpq}G(p;t|s)U(k;t|s)]ds \qquad (k >> q'), \tag{3.17}$$

which is obtained from (2.6) by neglecting the term involving $U(k;t|s)$ for $p < q'$ and assuming that the characteristic times of mode q are long compared to those of k and p. The factor 2 in the first term on the right-hand side of (3.17) comes from including the contributions of both $q < q'$ and $p < q'$ in the first term on the right-hand side of (2.6). There is a cancellation between the A and B terms in (3.17) to leading order in p-k. The remainder can be evaluated conveniently by considering symmetrical and antisymmetrical parts as in obtaining (3.15). The final result can be written

$$T_{<q}(k,t) = -2[\int_0^q E(p,t)p^2dp]\frac{\partial}{\partial k}\left[\nu_k(t) + \frac{2\pi}{15}k^4\Delta(k,t) - \frac{2\pi}{15}k^3\int_{t_0}^{t} G(k;t|s)U(k;t|s)ds\right] \qquad (k >> q). \tag{3.18}$$

The three terms in (3.18) are most easily interpreted by integrating over k to form the corresponding contribution to $\Pi(k,t)$:

$$\Pi_{<q}(k,t) = 2\int_0^q E(p,t)p^2dp[\nu_k(t) + \frac{2\pi}{15}k^4\Delta(k,t)$$

$$- \frac{2\pi}{15}k^3\int_{t_0}^{t} G(k;t|s)U(k;t|s)ds] \qquad (k >> q). \tag{3.19}$$

The first term on the right clearly corresponds to the loss from low wavenumbers given by (3.14). If the modes $\sim k$ were in equipartition equilibrium among themselves, they would satisfy the relations[1]

$$G(k;t|s) = R(k;t|s), \qquad \partial U(k;t|t)/\partial k = 0, \tag{3.20}$$

whence $\Delta(k,t)$ would vanish. On the other hand, if $U(k;t|t)$ is a rapidly decreasing function of k, as in the inertial range, $\Delta(k,t)$ is positive. Its appearance in (3.19) then represents a net transfer of energy from modes in the range (k-q, k) to modes >k due to straining by modes <q but without net loss from the modes <q. The last term in (3.19) survives even if the modes $\sim k$ are in equipartition. Equation (2.6) is easily shown to give zero transfer among a triad all three of whose members are in equipartition equilibrium. This may be called the detailed balance property. The presence of the last term in (3.19) illustrates that detailed balance between only two members of a conservative interacting triad of modes is an invalid concept.

The eddy viscosity (3.15) does not have the form proposed by Heisenberg[3], but it gives qualitatively similar results in the inertial range. There it yields $\nu_q \sim [q^{-1}E(q)]^{1/2}$, as the analysis to follow will show.

When viscosity effects are strong, the characteristic fall-off time of $G(q;t|s)$ is $(\nu q^2)^{-1}$, and the result is a value of ν_q which is smaller than Heisenberg's and inversely proportional to the molecular viscosity. The absence of an interference between molecular and eddy viscosities in Heisenberg's formula leads to the prediction of a power-law dissipation-range spectrum, which implies non-existence of high-order spatial derivatives of the velocity field.[4,5]

The asymptotic formula for $T_{<q}(k,t)$ indicates that energy transfer associated with widely separated wavenumbers is proportional to the mean-square vorticity in the lower wavenumbers. It is important in understanding the structure of (2.6) to remember that this result involves a near cancellation between the two terms on the right-hand side. These terms separately give contributions proportional to the energy in the wavenumbers $<q$, not to the mean-square vorticity. The term containing $G(k;t|s)$ is an input term giving a positive contribution to $T(k,t)$, while the term containing $U(k;t|s)$ is an output term representing a drain of energy from mode k to other modes. The input and output contributions from low wavenumbers are proportional to energy because they represent convection as well as straining. Convection of high-wavenumber structures by strongly excited low-wavenumber velocity components implies a rapid change of phase of the high-wavenumber Fourier amplitudes; that is to say, a rapid exchange of energy between sine and cosine components of the high wavenumbers. This exchange is represented in (2.6) by the large, cancelling input and output contributions. The net contribution $T_{<q}(k,t)$ represents the effect of straining alone.

Since the output integral in (2.6) involves $U(k;t|s)$, it gives a negative contribution to $T(k,t)$ roughly proportional to $E(k,t)$. As a result, the general behavior of (2.6) is to give energy flow out of strongly excited modes into weakly excited modes. In equipartition, the input and output terms cancel exactly. This can be seen immediately by using (3.20) in (2.6), as noted earlier. Out of equipartition, the energy flow is from low to high wavenumbers only if $U(k;t|t)$ decreases as k increases.

4. THE TIME-CORRELATION AND RESPONSE EQUATIONS

The multiplicity of terms in (2.7) and (2.8) arises from the peculiar way in which Lagrangian dynamics are represented through (1.2). A more standard Lagrangian analysis[6] is based on the equation for the particle acceleration $\partial \underset{\sim}{u}(\underset{\sim}{x},t_0|r)/\partial r$. This treatment leads to trouble in turbulence theory because the expressions for viscous and pressure forces involve awkward nonlinearity, which so far has precluded approximate statistical equations that preserve incompressibility and conserve energy. In the present approach, this trouble is sidestepped by avoiding direct calculation of $\partial \underset{\sim}{u}(\underset{\sim}{x},t|r)/\partial r$. Instead, the basic equations are for $\partial \underset{\sim}{u}(\underset{\sim}{x},t|t)/\partial t$ and $\partial \underset{\sim}{u}(\underset{\sim}{x},t|r)/\partial t$. The r dependence is determined by the difference between the behaviors along the appropriate paths of integration of these two equations. The different approaches are illustrated in Fig. 1. Suppose that the initial Eulerian field $\underset{\sim}{u}(\underset{\sim}{x},t_0) = \underset{\sim}{u}(\underset{\sim}{x},t_0|t_0)$ is given and $\underset{\sim}{u}(\underset{\sim}{x},t_0|r)$ is desired. The straightforward procedure is to integrate

$\partial \underset{\sim}{u}(\underset{\sim}{x},t_0|r)/\partial r$ along the path AB. In the present treatment, the Navier-Stokes equation is integrated along AC, yielding $\underset{\sim}{u}(\underset{\sim}{x},t|t)$ for $t_0 \le t \le r$. Then (1.2) is integrated backward in t along CB. Thus $\underset{\sim}{u}(\underset{\sim}{x},t_0|r)-\underset{\sim}{u}(\underset{\sim}{x},t_0|t_0)$, the total change in the particle velocity during the interval (t_0, r), appears as the difference between the two forward integrations AC and BC. If there are no viscous, pressure, or external forces, the two integrations are identical, so that $\underset{\sim}{u}(\underset{\sim}{x},t_0|r)-\underset{\sim}{u}(\underset{\sim}{x},t_0|t_0) = 0$.

Since $(\underset{\sim}{x},t)$ is laboratory spacetime, this amounts to describing Lagrangian behavior by equations which are Eulerian in character, a fact pointed out to the author by Prof. S. Corrsin. The advantage is that conservation and invariance properties appear directly and are easily incorporated in the final closure equations. The penalty is that the Lagrangian statistical functions are determined as algebraic sums of a multiplicity of intricately counterbalancing terms.

The meaning of the various terms in (2.7) can be uncovered by tracing how they arise in the perturbation analysis[1] through which the equation was derived. The ν term has an obvious significance: simple viscous decay of Fourier amplitude of the Eulerian field at time t. The first term on the right-hand side can be interpreted by considering a hypothetical situation. Imagine that a velocity field with an isotropic, multivariate-Gaussian ensemble distribution is set up at time r and then forces are somehow applied so that the Eulerian field is frozen thereafter, exhibiting no time-dependence at all. The fluid particles move along the streamlines of the spatially varying Eulerian field, and the Lagrangian velocities change with time. If the derivation of (2.7) is repeated for this situation,

the only surviving term is the first term on the right-hand side. This term represents a decrement in the correlation $U(k;t|r)$ due to the labeling transformation (transformation from Eulerian to Lagrangian coordinates): The particle at $\underset{\sim}{x}$ at time t was elsewhere at time r, so that $\underset{\sim}{u}(\underset{\sim}{x},t|r)$ is really the Eulerian velocity at a point other than $\underset{\sim}{x}$ and is partly decorrelated with $\underset{\sim}{u}(\underset{\sim}{x},t|t)$.

In the actual case, where the Eulerian velocity is not static, this correlation loss is partly compensated by a correlation of the relabeling with the evolution of the Eulerian field during the same period: The substantial derivative $[\partial/\partial t + \underset{\sim}{u}(\underset{\sim}{x},t)\cdot\underset{\sim}{\nabla}]$ which determines the relabeling also appears in the Navier-Stokes equation. The second term on the right-hand side of (2.7) expresses the compensation. The first and second terms together express net effects of relabeling during the period (r,t). Call them the Class I terms.

The remaining terms on the right-hand side of (2.7) all express correlations arising from the distortion of the Eulerian field over its entire history from t_0. They consist of Class II, with upper limit r, and Class III, with upper limit t. Each of these classes is itself a sum of compensating terms. The algebraic sum of the terms within each class provides a cancellation which eliminates convection effects in the Eulerian evolution; only the difference between the histories at different space points makes up the net contribution. The integrals of Class II and Class III over d^3k separately vanish for all t and r. This expresses that past nonlinear processes in the Eulerian field have no direct effect on $\partial\langle\underset{\sim}{u}(\underset{\sim}{x},t|t)\cdot\underset{\sim}{u}(\underset{\sim}{x},t|r)\rangle/\partial t$. The latter derivative is determined wholly by

the labeling transformation in the interval (r,t). The vanishing of the integrals over d^3k can be verified by using (2.9), (3.4), and some changes of variable.

It may be asked why the net effect of past distortion of the Eulerian field does not appear simply as an integral over the interval (r,t) instead of as the algebraic sum of Class II integrals over (t_0,r) and Class III integrals over (t_0,t). The reason is that distortion during (r,t) is affected by higher correlations built up over the entire history of the dynamical interaction as well as by the value of the velocity covariance at time r. It will be seen below that, in general, the Class II and Class III terms do not cancel each other if t = r. They express effects that exist even if no labeling transformation has taken place.

A similar analysis may be made for the response equation (2.8). The first two terms on the right-hand side arise from relabeling associated with the unperturbed velocity field; that is, relabeling of the perturbation according to the transformation that would take place in absence of perturbation. They are analogous to the Class I terms in (2.7). In addition, the applied perturbation at time r, to which $G(k;t|r)$ gives the average response, induces a perturbation in the relabeling transformation. This is expressed by the $[D_{kpq} - B_{kpq}]_{\Lambda}^{\text{term}}$ on the right-hand side of (2.8). The remaining two terms represent effects from the perturbation in the nonlinear evolution of the Eulerian field.

Hopefully, the interpretations above help a little to make (2.7) and (2.8) intelligible. However, no clean-cut separation is possible among the various effects cited. All the terms together determine the values of the G and U functions which appear in any one term.

It was stated in Sec. 1 that $\langle \underset{\sim}{u}(\underset{\sim}{x},t|t)\cdot\underset{\sim}{u}(\underset{\sim}{x}',t|r)\rangle$ was not symmetric about $r = t$ in stationary, homogeneous turbulence, except if $\underset{\sim}{x} = \underset{\sim}{x}'$. This can be investigated with (2.7). First, an isotropic energy source is needed in order that stationarity and isotropy be mutually consistent. The easiest way is to add a negative damping term to the Navier-Stokes equation so that, after Fourier transformation,

$$\nu k^2 \to \nu k^2 - \mu(k), \tag{4.1}$$

where $\mu(k)$ is positive, and $>\nu k^2$ for some k. Let $u(k)$ vanish outside the energy-containing range. This input mechanism may be regarded as an idealization of the mechanism by which real turbulence draws energy from an overall shear. The effect of the input on (2.6)-(2.8) is simply to replace νk^2 by $\nu k^2 - \mu(k)$ everywhere. To describe the stationary state, the limit $t_0 \to -\infty$ is taken.

Now consider (2.7) for $r = t$. The two D' terms cancel exactly, and, by (2.9) and the symmetry of the integrand factors in p and q, the coefficient D_{kpq} in the sixth term can be replaced by B_{kpq}. The first two terms on the right-hand side vanish. The result is that the right-hand side is identical with the right-hand side of (2.6). Now subtract (2.6) from twice (2.7) and multiply by $2\pi k^2$. In the stationary state, $\partial U(k;t|t)/\partial t = 0$. Therefore, by the definitions of $T(k,t)$ and $R(k;t|r)$, the result is

$$E(k,t)[\partial R(k;t|r)/\partial t]_{r=t} = \frac{1}{2}\, T(k,t),$$

or, by stationarity,

$$E(k,t)[\partial R(k;t|r)/\partial r]_{r=t} = -\frac{1}{2}\, T(k,t). \tag{4.2}$$

Fourier transformation of (4.2) yields

$$[\partial U_{ii}(\underset{\sim}{x},t|t;\underset{\sim}{x}+\underset{\sim}{y},t|r)/\partial r]_{r=t} = -\int_0^\infty T(k,t)\frac{\sin(ky)}{ky}\,dk. \qquad (4.3)$$

For y = 0, (4.3) gives zero slope at r = t, by (3.3). For y intermediate between energy-containing and dissipation scales, the sin(ky)/(ky) factor depresses the relative contribution of wavenumbers receiving energy, so that the right-hand side of (4.3) is positive. This agrees with the discussion in Sec. 1. Equation (4.3) shows that wavenumbers where energy is fed in [negative T(k,t)] contribute acceleration positively correlated with particle velocity, while wavenumbers dissipating energy contribute negatively correlated acceleration.

Equation (4.2) actually is an exact result of stationarity, independent of the closure approximation and of the nature of the input forces. If an isotropic, statistically stationary forcing term of any kind is added to the Navier-Stokes equation, then (4.2) follows immediately from the identity of the triple moments and input terms in the exact equations for $\partial U(k;t|t)/\partial t$ and $[\partial U(k;t|r)/\partial t]_{r=t}$ that can be formed from (1.2) and the Navier-Stokes equation.

Evenness of $U_{ii}(\underset{\sim}{x},t|t;\underset{\sim}{x},t|r)$ as a function of r-t requires that all the higher odd r derivatives vanish at r = t, as well as the first. The behavior of the higher derivatives has not been determined for either (2.6)-(2.8) or the unabridged LHDI equations. This question is part of the general problem of integrability and realizability of the LHDI equations discussed in Ref. 1.

Further insight about the time-correlation and response equations is

provided by investigating the contributions from interactions with much larger and much smaller wavenumbers. It is interesting first to examine the contribution from very local interactions, $p \approx k$, $q \approx k$. Suppose that all triad interactions are absent from (2.6)-(2.8) except those for which

$$|p - k| \le \delta, \quad |q - k| \le \delta, \quad \delta << k. \tag{4.4}$$

Let δ be small enough that p and q may be replaced by k everywhere in the integrands. Then

$$B_{kpq} \approx D_{kpq} \approx D'_{kpq} \approx \frac{3}{8}\pi k^3, \qquad C_{kpq} \approx \frac{3}{4}\pi k^3. \tag{4.5}$$

The right-hand side of (2.6) vanishes to this approximation; because of symmetry, very local interactions produce no net energy transfer. All terms but the first two in the right-hand sides of (2.7) and (2.8) either cancel in pairs or vanish. When the integrations over p and q are performed, the net contributions from the first two terms yield

$$(\partial/\partial t + \nu k^2)U(k;t|r) = -\frac{3\pi}{2} k^3\delta^2 U(k;t|r)\int_r^t U(k;t|s)ds, \tag{4.6}$$

$$(\partial/\partial t + \nu k^2)G(k;t|r) = -\frac{3\pi}{2} k^3\delta^2 G(k;t|r)\int_r^t U(k;t|s)ds,$$

$$G(k;r|r) = 1. \tag{4.7}$$

The exact solution to (4.6) and (4.7) for $\nu = 0$ can be obtained by the trial substitution

$$U(k;t|r) = U(k)G(k;t|r) = g(t-r)U(k), \tag{4.8}$$

which reduces (4.6) and (4.7) to the single equation

$$\partial g(t)/\partial t = -a^2 g(t)\int_0^t g(s)ds, \qquad g(0) = 1, \tag{4.9}$$

where $a^2 = (3\pi/2)k^3\delta^2 U(k)$. The solution of (4.9) is

$$g(t) = 4e^{-at\sqrt{2}}/(1 + e^{-at\sqrt{2}})^2, \tag{4.10}$$

which is an even function of t and has the asymptotic behavior

$$g(t) \approx 1 - \tfrac{1}{2}(at)^2 \quad (at<<1), \quad g(t) \approx 4e^{-at\sqrt{2}} \quad (at>>1). \tag{4.11}$$

This solution suggests that interactions local in wavenumber tend to produce an eventual rapid decay of $U(k;t|r)$ and $G(k;t|r)$ at large t-r. Setting $\delta = k$ suggests that the characteristic decay frequency due to interactions with wavenumbers of order k is crudely kv_k, where $v_k^2 = kE(k,t)$.

To obtain the contribution to (2.7) from all interactions involving wavenumbers $\geq q >> k$, make the same assumptions used in obtaining (3.10). The asymptotic contribution is

$$[\partial U(k;t|r)/\partial t]_{>q} = -U(k;t|r)\int_q^\infty dq' \int_{q'-k}^{q'+k} dp\, C_{kpq'} \int_r^t U(q';t|s)ds$$

$$+ B_{kpq'} \int_{t_0}^t G(p;t|s)U(q';t|s)ds] \quad (q>>k). \tag{4.12}$$

All the other terms on the right-hand side are suppressed either because they involve U(p)U(q) or because they involve at least one function for p or q with a time separation of order t-r; (4.12) assumes that t-r is large compared to the characteristic decay times of the modes $\geq q$. In the second term of (4.12), $U(k;r|s) \approx U(k;r|t) = U(k;t|r)$ has been used, because only $s \approx t$ can contribute. The wavenumber integrations in this term were performed in evaluating (3.10). The integration in the first term is easily performed, with the result

$$[\partial U(k;t|r)/\partial t]_{>q} = -\nu_q'(t)U(k;t|r) \qquad (q >> k),$$

$$\nu_q'(t) = \nu_q(t) + \frac{4\pi}{3}\int_q^\infty dq' \int_{t_0}^t (q')^2 U(q';t|s)ds. \tag{4.13}$$

In the expression for $\nu_q'(t)$, the lower limit r has been changed to t_0. This is permissible because all appreciable contribution comes from $t-s << t-r$. Similar analysis gives

$$[\partial G(k;t|r)/\partial t]_{>q} = -\nu_q'(t)G(k;t|r) \qquad (q >> k) \tag{4.14}$$

for the contribution to the right-hand side of (2.8) from wavenumbers $\geq q$, for t-r large compared to the characteristic times of these wavenumbers.

Comparison of (4.13) and (4.14) with the viscous terms in (2.7) and (2.8) shows that the high-wavenumber interactions act like an eddy viscosity, but not the same eddy viscosity which appears in the energy-transfer contribution (3.14). The difference may be understood as follows. The energy transfer among different wavenumbers in isotropic turbulence can be ascribed to advective straining. The pressure term makes no direct contribution. The pressure term also makes no direct contribution to the evolution of the Eulerian time covariance $\langle \underset{\sim}{u}(\underset{\sim}{x},t)\cdot\underset{\sim}{u}(\underset{\sim}{x}',t')\rangle$. The exact equation for this covariance is

$$(\partial/\partial t - \nu\nabla_x^2)\langle \underset{\sim}{u}(\underset{\sim}{x},t)\cdot\underset{\sim}{u}(\underset{\sim}{x}',t')\rangle = -\langle \underset{\sim}{u}(\underset{\sim}{x},t)\cdot\underset{\sim}{\nabla}_x\underset{\sim}{u}(\underset{\sim}{x},t)\cdot\underset{\sim}{u}(\underset{\sim}{x}',t')\rangle$$
$$-\langle \underset{\sim}{u}(\underset{\sim}{x}',t')\cdot\underset{\sim}{\nabla}p(\underset{\sim}{x},t)\rangle, \tag{4.15}$$

and the term containing the pressure $p(\underset{\sim}{x},t)$ vanishes by incompressibility and homogeneity.

Just the reverse is true for the Lagrangian time covariance. Advection

produces no direct change in particle velocity and therefore makes no direct contribution to decay of the Lagrangian covariance. The pressure fluctuations, on the other hand, produce accelerations which decorrelate the Lagrangian velocity. Crudely speaking, $\nu_q(t)$ may be called the eddy viscosity due to advective straining and $\nu'_q(t)$, the eddy viscosity due to pressure fluctuations. The separation is not clean because the advection and pressure fluctuations react on each other.

The difference $\nu'_q(t) - \nu_q(t)$ is a positive integral. This provides a crude suggestion that the Lagrangian correlation time for turbulence may be shorter than the Eulerian correlation time. Some simple physical reasoning leads to the same suggestion.[7] The argument is that even in a frozen Eulerian velocity field (infinite Eulerian correlation time), Lagrangian covariances decay with difference time because given fluid elements migrate through the velocity field. This question will be discussed further in Sec. 6, after the quantitative inertial-range results are available.

Now consider the contributions to (2.7) and (2.8) from interactions with wavenumbers $\leq q' << k$. For t-r the order of the correlation and response times of mode k, the situation is like that for energy transfer. The contributions to the various terms on the right-hand sides cancel in such fashion that what remains is proportional to the mean-square vorticity in the wavenumbers $\leq q'$. In (2.7), the Class I, Class II, and Class III$_\Lambda^{\text{terms}}$ cancel separately. In (2.8), there are cancellations between the first two terms, within the third term, and between the last two terms.

The behavior at large t-r is more complicated. The analysis above

suggests that if k interacted only with wavenumbers of order k and larger, the functions $U(k;t|r)$ and $G(k;t|r)$ would fall off exponentially for large t-r. What actually happens is that interactions with low wavenumbers dominate the long-time behavior and cause these functions to fall off more slowly. Discussion of this phenomenon is postponed to Sec. 6.

5. INERTIAL-RANGE EQUATIONS

Kolmogorov's inertial-range law is

$$E(k) = C\varepsilon^{2/3}k^{-5/3}, \tag{5.1}$$

where ε is the rate of energy dissipation per unit mass and C is a universal constant. The time-dependence is omitted in (5.1) because the relevant dynamical times in the inertial range are assumed to be short compared to the decay time of the total turbulent energy, so that the inertial range is nearly statistically stationary. Kolmogorov's hypotheses also yield inertial-range forms for $G(k;t|r)$ and $R(k;t|r)$. The requirement that they depend only on ε, k, and t-r imposes on these functions the forms

$$G(k;t|r) = G(\varepsilon^{1/3}k^{2/3}\tau), \quad R(k;t|r) = R(\varepsilon^{1/3}k^{2/3}\tau), \quad \tau = t-r. \tag{5.2}$$

Reference 1 argued that the LHDI equations led to a Kolmogorov inertial range because they gave the required localness of the dynamical interaction in wavenumber. This can be verified for the abridged LHDI equations by substituting (5.1) and (5.2) into (2.6)-(2.8) and checking that the integrations over p and q converge properly at zero and infinite wavenumbers. The equations for $G(\tau)$ and $R(\tau)$ which result from the substitution can be

written most usefully by introducing rescaled functions

$$\overline{G}(\tau) = G(\gamma\tau), \qquad \overline{R}(\tau) = R(\gamma\tau), \qquad \gamma = (2\pi/C)^{1/2}, \tag{5.3}$$

where, for convenience, τ now denotes the nondimensional argument $\epsilon^{1/3}k^{2/3}\tau$ of (5.2). Then C drops out of (2.7) and (2.8) leaving

$$d\overline{G}(\tau)/d\tau = \iint_{\Delta} dvdw\{-C_{vw}\overline{G}(\tau)\int_0^{\tau}\overline{R}(w^{2/3}s)ds + D_{vw}\overline{G}(v^{2/3}\tau)\int_0^{\tau}\overline{R}(w^{2/3}s)ds$$

$$- [D_{uv} - B_{uv}]\overline{G}(v^{2/3}\tau)\overline{R}(w^{2/3}\tau)\int_0^{\tau}\overline{G}(s)ds$$

$$- \int_0^{\tau}[B_{vw}\overline{G}(v^{2/3}s)\overline{G}(\tau-s) - D'_{vw}\overline{G}(s)\overline{G}(v^{2/3}(\tau-s))]\overline{R}(w^{2/3}s)ds\}$$

$$(\tau \geq 0), \ \overline{G}(0) = 1, \tag{5.4}$$

$$d\overline{R}(\tau)/d\tau = \iint_{\Delta} dvdw\{-C_{vw}\overline{R}(\tau)\int_0^{\tau}\overline{R}(w^{2/3}s)ds + D_{vw}v^{-11/3}\overline{R}(v^{2/3}\tau)\int_0^{\tau}\overline{R}(w^{2/3}s)ds$$

$$+ \int_{\tau}^{\infty}[B_{vw}v^{-11/3}\overline{G}(s-\tau)\overline{R}(v^{2/3}s) - D'_{vw}\overline{G}(v^{2/3}(s-\tau))\overline{R}(s)]\overline{R}(w^{2/3}s)ds$$

$$- \int_0^{\infty}[B_{vw}\overline{G}(v^{2/3}s)\overline{R}(|s-\tau|) - D_{vw}v^{-11/3}\overline{G}(s)\overline{R}(v^{2/3}|s-\tau|)]\overline{R}(w^{2/3}s)ds$$

$$- \int_0^{\infty}[B_{vw} - D'_{vw}]\overline{G}(v^{2/3}s)\overline{R}(s)\overline{R}(w^{2/3}|s-\tau|)ds\} \quad (\tau \geq 0), \quad \overline{R}(0) = 1. \tag{5.5}$$

Here $v = p/k$, $w = q/k$, and $\iint_{\Delta}$ now denotes integration over all of the (v,w) plane such that $(1,v,w)$ can form the sides of a triangle. In accord with the assumption of an asymptotically stationary inertial range, the limit $t_0 \to -\infty$ has been taken. In addition, some simple transformations of time variables have been made and the symmetry property (2.5) has been used.

The coefficients in (5.4), (5.5) can be written

$$B_{vw} = \pi v^2 w^{-8/3}(xy + z^3), \quad C_{vw} = \pi v w^{-8/3}(1 - y^2),$$

$$D_{vw} = \frac{1}{2}\pi v w^{-8/3}(1 - xyz - 2y^2z^2 + z^2 - y^2),$$

$$D'_{vw} = \frac{1}{2}\pi v^3 w^{-8/3}(1 - xyz - 2x^2z^2 + z^2 - x^2), \qquad (5.6)$$

where x, y, z are now the cosines of the interior angles opposite the triangle sides l, v, w respectively.

Substitution of (5.1) and (5.2) into (2.6) makes T(k,t) vanish identically by virtue of the conservation identity (3.4). The energy gained by k from lower modes is exactly balanced by a drain to higher modes. This formal result is a necessary consistency requirement for an inertial range, but it says nothing about the localness of the energy transfer. Transfer between widely separated wavenumbers can be investigated by substituting (5.1) and (5.2) into (3.15) and (3.19). The result is that both the loss from modes $\leq q$ due to interactions with modes $\geq k$ and the gain in modes $\geq k$ due to interactions with modes $\leq q$ are $\propto (q/k)^{4/3}$ for $k >> q$, provided that $G(\tau)$ and $R(\tau)$ are properly integrable over τ. Discussion of the behavior of the latter functions, and the check of localness for (5.4) and (5.5), are discussed later in this Section and in Sec. 6.

The Kolmogorov constant C can be determined by evaluating (3.8). In the inertial range, $\Pi(k,t)$ must be independent of k and equal to ε, since there is negligible dissipation and the energy cascade is conservative. This implies the similarity law

$$T(ak, ap, aq, t) = a^{-3}T(k, p, q, t), \qquad (5.7)$$

where a is such that all wavenumbers involved are in the inertial range. Equation (5.7) can be verified for the abridged LHDI transfer function by inserting (5.1) and (5.2). It leads to an important simplification of (3.8). Write $b = p'k/k'$, $q = q'k/k'$ so that the expression for $\varepsilon = \Pi(k,t)$ becomes

$$\varepsilon = \int_k^\infty (k/k')dk' \int_0^{k^2/k'} db \int_{b_*}^{b+k} dqT(k,b,q) \quad (b_* = \text{larger of } b,\ k-b), \tag{5.8}$$

by (5.7). The time argument in (5.8) and later equations is suppressed as in (5.1). Now set $p = k^2/k'$ in (5.8) and find

$$\varepsilon = \int_0^k (k/p)dp \int_0^p db \int_{b_*}^{b+k} dqT(k,b,q). \tag{5.9}$$

Finally, integrate by parts and obtain[8]

$$\varepsilon = k \int_0^k dp\ \ln(k/p) \int_{p_*}^{p+k} T(k,p,q)dq. \tag{5.10}$$

If (5.1) and (5.2) are substituted into (5.10), some simple changes of variable yield the formula

$$(C/2\pi)^{-3/2} = 4\pi \int_0^1 dv\ \ln(1/v) \int_{v_*}^{1+v} dw \int_0^\infty ds[A_{vw}\bar{G}(s)\bar{R}(v^{2/3}s)\bar{R}(w^{2/3}s)$$

$$-B_{vw}\bar{G}(v^{2/3}s)\bar{R}(s)\bar{R}(w^{2/3}s) - B_{wv}\bar{G}(w^{2/3}s)\bar{R}(s)\bar{R}(v^{2/3}s)], \tag{5.11}$$

where

$$A_{vw} = (B_{1vw} + B_{1wv})(vw)^{-8/3}, \quad v_* = \left|v - \tfrac{1}{2}\right| + \tfrac{1}{2}.$$

It should be remembered that although $T(k,t)$ vanishes identically in the inertial range, $\Pi(k,t)$ defined by (3.7) does not vanish, because the integrations include the dissipation range. The passage from (3.7) to (3.8) uses the conservation properties to obtain a formula for C which involves only inertial-range functions.

Equation (5.10) can be cast into the form

$$\varepsilon = \int_1^\infty W(\alpha)\frac{d\alpha}{\alpha}\,, \tag{5.12}$$

where $W(\alpha)(d\alpha/\alpha)$ is defined as the contribution to ε from all triad interactions such that the ratio of maximum to minimum wavenumber lies between α and $\alpha + d\alpha$. To obtain $W(\alpha)$, write (5.10) as

$$\varepsilon = k\int_0^k dp\ \ln(k/p)\int_{p_*}^k T(k,p,q)dq + k\int_0^k dp\ \ln(k/p)\int_k^{k+p} T(k,p,q)dq.$$

In the first term the ratio of maximum to minimum wavenumber is $\alpha = k/p$ and in the second term it is $\alpha = q/p$. In the first term write $q = k/\beta$ and in the second write $p = k/\beta$, $q = \alpha k/\beta$. Then some manipulations of the limits yields ε in the form (5.12) with

$$W(\alpha) = k^3[\alpha^{-1}\ln\alpha\int_1^{\alpha^*} T(k,k/\alpha,k/\beta)\beta^{-2}d\beta + \alpha\int_{\alpha-1}^{\alpha} T(k,k/\beta,\alpha k/\beta)\beta^{-3}\ln\beta\ d\beta],$$

$$\alpha^* = [\,|\tfrac{1}{\alpha} - \tfrac{1}{2}| + \tfrac{1}{2}\,]^{-1}, \tag{5.13}$$

which is independent of k, by (5.7). Substitution of (5.1) and (5.2) into (5.13) yields

$$W(\alpha) \propto \alpha^{-4/3} \qquad \alpha >> 1, \tag{5.14}$$

in agreement with the results obtained from (3.15) and (3.19).

For values of τ small enough that $\overline{R}(\tau)$ and $\overline{G}(\tau)$ are still O(1), the convergence properties of the wavenumber integrals in (5.4) and (5.5) are like those of the energy transfer. Equations (4.13) and (4.14) yield contributions $\propto\alpha^{-4/3}$ from interactions with v or w > α, $\alpha >> 1$. Investigation shows that the contribution from interactions involving v or w $<\alpha^{-1}$ is $\propto\alpha^{-4/3}$ also. The behavior at large τ will be discussed in Sec. 6.

6. BASIC NUMERICAL RESULTS AND THEIR INTERPRETATION

Before inertial-range computations were attempted, an overall consistency check of the closure equations was performed by repeating some numerical studies originally carried out for the unaltered Eulerian direct-interaction equations.[9] Inviscid equipartition solutions were investigated first. The viscosity was set equal to zero in (2.6)-(2.8) and the equations truncated to a finite wavenumber range, as in Ref. 9. Initial spectra $U(k;t_0|t_0)$ of several forms were taken, including sharply peaked spectra confined to a narrow wavenumber band. The system was found to approach equipartition and fluctuation-dissipation equality [Eq.(3.20)]. $E(k,t)$ stayed positive for all k and t, and $G(k;t|r)$ and $R(k;t|r)$ approached zero for large t-r. Some of the finite-viscosity decay calculations at moderate Reynolds number described in Ref. 9 were also repeated. The spectral predictions of the present abridged LHDI equations turned out to be qualitatively similar to those of the unaltered Eulerian direct-interaction equations at the Reynolds numbers investigated ($R_\lambda \lesssim 40$).

The unaltered direct-interaction equations are the exact description of a model dynamical system and are guaranteed self-consistent. There is no such guarantee for the LHDI equations.[1] The numerical results just described, and those to follow, suggest that the LHDI equations actually are a more stable system than the unaltered direct-interaction equations and stay farther from unphysical behavior. Functions which decay with damped oscillations in the unaltered approximation instead fall smoothly to zero in the LHDI and abridged LHDI approximations. A possible explanation lies in the general nature of the alteration prescription. The change from

direct-interaction to LHDI triple-moment formulas consists of replacing certain labeling times $s < t$ by t in the integrals over the history of the fluid. This appears to be stabilizing in the same way as a change from forward to backward differences can be stabilizing in the numerical integration of differential equations.

The basic inertial-range equations (5.4) and (5.5) were integrated by a modification of numerical methods developed for the Eulerian direct-interaction equations.[9] The Kolmogorov constant was then computed by evaluating the multiple integral (5.11) in such a way that the calculation also yielded $W(\alpha)$ without extra work. The results for G, R, W, and

$$P(\alpha) \equiv \int_1^\alpha W(\alpha')\frac{d\alpha'}{\alpha'}$$

are plotted in Figs. 2 and 3. The value computed for the Kolmogorov constant is[10]

$$C = 1.77. \tag{6.1}$$

A description of the numerical procedures and estimates of computational errors are given in the Appendix.

The following values for integrals over R and G were obtained:

$$I_G = \int_0^\infty G(s)ds = 1.04, \quad I_R = \int_0^\infty R(s)ds = 1.87, \quad I_1 = \int_0^\infty G(s)R(s)ds = 0.76,$$

$$I_2 = \int_0^\infty [R(s)dG(s)/ds - G(s)dR(s)/ds]sds = -0.19. \tag{6.2}$$

These numbers yield the following inertial-range values for the quantities which appear in (3.15), (3.18), and (4.13):

$$\nu_k = \frac{1}{6}[I_1 - \frac{1}{5} I_2]C\ \varepsilon^{1/3}k^{-4/3} = 0.235\ \varepsilon^{1/3}k^{-4/3},$$

$$\frac{14\pi}{15}\int_k^\infty p^2 dp \int_{-\infty}^t G(p;t|s)U(p;t|s)ds = \frac{7}{20} CI_1\ \varepsilon^{1/3}k^{-4/3} = 0.47\ \varepsilon^{1/3}k^{-4/3},$$

$$\frac{2\pi}{15}\int_k^\infty p^3\Delta(p)dp = \frac{1}{60}[11I_1 + 2I_2]C\ \varepsilon^{1/3}k^{-4/3} = 0.235\ \varepsilon^{1/3}k^{-4/3},$$

$$\frac{2\pi}{15} k^4\Delta(k) = \frac{1}{45}[11I_1 + 2I_2]C\ \varepsilon^{1/3}k^{-4/3} = 0.314\ \varepsilon^{1/3}k^{-4/3},$$

$$\frac{2\pi}{15} k^3\int_{-\infty}^t G(k;t|s)U(k;t|s)ds = \frac{1}{15} CI_1\ \varepsilon^{1/3}k^{-4/3} = 0.090\ \varepsilon^{1/3}k^{-4/3},$$

$$\nu_k' = \nu_k + \frac{1}{2} CI_R\ \varepsilon^{1/3}k^{-4/3} = 1.89\ \varepsilon^{1/3}k^{-4/3}. \qquad (6.3)$$

Figure 3 indicates that $W(\alpha)$ peaks at $\alpha = 2$. However, it also indicates that only about 20% of the total transfer comes from $\alpha \leq 2$; that is, from triad interactions in which the largest and smallest wavenumbers differ by a factor of two or less. The tail of $W(\alpha)$ carries most of the energy transfer, so that the local cascade appealed to by Kolmogorov seems actually to be rather diffuse. This may mean that inertial ranges must be quite extensive before they exhibit nearly asymptotic dynamical properties. The numerical results support the $\alpha^{-4/3}$ dependence of $W(\alpha)$ at large α found analytically.

The numerical results (6.3) for effective eddy viscosities and other functions relevant to distant interactions exhibit some interesting features. Substitution of these results into (3.19) indicates that the eddy-viscosity loss from low wavenumbers (the first term on the right-hand side) represents slightly more than 50% of the energy gain of the high wavenumbers. An

almost equal gain in the wavenumbers >k comes from the straining action of the wavenumbers ≤q upon wavenumbers in the range (k-q, k), without loss from the wavenumbers ≤q.

The most striking feature of (6.3) is that ν_k' is about eight times as large as ν_k. Some help in interpretation comes from noting that $\nu_k' - \nu_k$ arises from the first term on the right-hand side of (2.7), or (2.8). According to the discussion in Sec. 4, this term would contribute all of ν_k' if the Eulerian field were frozen. The remaining contribution ν_k represents the effects of change of the Eulerian field with time. A large ratio of ν_k' to ν_k means that the migration of particles, under the action of wavenumbers ≥k, is accompanied by accelerations which leave the large-scale Eulerian field almost unchanged; the particles are subjected to pressure forces such that they take on nearly the velocity of their new surroundings, apart from fluctuations at scales $\leq k^{-1}$. In other words, the transport of <u>particles</u> by the velocity excitation in wavenumbers ≥k is much more efficient than the transport of <u>momentum</u> across gradients of the large-scale velocity field.

The migration of fluid particles is directly related to the turbulent transport of heat in a fluid with passive temperature gradients. A large ratio ν_k'/ν_k therefore implies that the ratio of eddy conductivity to eddy viscosity is large. The LHDI result for the asymptotic thermometric eddy conductivity due to wavenumbers >k is, in fact, just $\nu_k' - \nu_k$. Thus (6.3) implies that the eddy-transport Prandtl number is

$$\sigma_k = \nu_k/(\nu_k' - \nu_k) = 0.14 \qquad \text{(inertial-range k)}. \tag{6.4}$$

Both $G(\tau)$ and $R(\tau)$ have zero slopes at $\tau = 0$. The result for G is obvious from (5.4). The slope of R vanishes because the right-hand side

of (5.5) is proportional to the energy transfer if $\tau = 0$ [see (4.2)], and the latter vanishes in the inertial range. Figure 2 indicates that G and R are indistinguishable near the origin but are markedly different at large argument values. For $\tau \lesssim 1$, the numerical investigation supports the analytical result that the behavior of $G(\tau)$ and $R(\tau)$ is dominated by interactions local in wavenumber. The behavior at large τ turns out to be dominated by interactions with low wavenumbers. Analysis of this phenomenon requires investigating the asymptotic forms of all the terms on the right-hand sides of (5.4) and (5.5). Only the results and their physical interpretation will be described here.

Consider (5.5) first. The low-wavenumber contributions come from small v and small w. The small-w contributions turn out to be negligible for all τ. The dominant small-v contributions for large τ come from $v \gtrsim \tau^{-3/2}$ and appear in the second and sixth terms on the right-hand side of (5.5), both of which have the coefficient D_{vw}. These contributions act as a source term which supports $\overline{R}(\tau)$ against the effective eddy damping from v, w = O(1). The result is

$$\overline{R}(\tau) \sim \tau^{-2} \qquad (\tau >> 1), \tag{6.5}$$

apart from a factor which varies more slowly than any power of τ. In (5.4), the important contributions again come from $v \gtrsim \tau^{-3/2}$ and appear in the second and last terms on the right-hand side. They result in a tail

$$\overline{G}(\tau) \sim \tau^{-15/2} \qquad (\tau >> 1), \tag{6.6}$$

apart from a factor which varies more slowly than any power of τ. The numerical results for $\overline{R}$ and $\overline{G}$ are consistent with (6.5) and (6.6). The dominant con-

tributions to C, as given by (5.11), and to the integrals in (6.2), are all from values of the time-arguments such that $\overline{G}$ and $\overline{R}$ are dominated by interactions local in wavenumber.

The physical interpretation of the tails on R and G is interesting. Transfer of energy from low to high wavenumbers involves straining processes which produce relative displacements of fluid elements. Suppose that there is an initial excitation of the velocity field at wavenumber p and that this excitation is spatially distorted by the action of much higher wavenumbers at a time t_1. Apart from the effects of acceleration, spectrum changes can be produced just by the differential displacement. If the elements along some line in the fluid suffer displacement modulated at wavenumbers $\sim k$ ($k >> p$), then the resulting Eulerian velocity field will have a component at wavenumber k because elements which are equally spaced after the displacement were not equally spaced before displacement. Of course, there will be additional spectrum changes because the fluid elements suffer changes of velocity, but they turn out not to be relevant.

Now consider $\underset{\sim}{u}(\underset{\sim}{x},t|r)$ for $t > t_1$ and $r < t_1$. The field $\underset{\sim}{u}(\underset{\sim}{x},t|t)$ is the Eulerian field after distortion, and has a component $\underset{\sim}{k}$. The field $\underset{\sim}{u}(\underset{\sim}{x},t|r)$ is the Eulerian field before distortion, but relabeled according to the positions of the fluid elements after the distortion. Because of the modulated displacement, correlation in the velocity of a fluid element before and after distortion shows up as a correlation between the fields $\underset{\sim}{u}(\underset{\sim}{x},t|t)$ and $\underset{\sim}{u}(\underset{\sim}{x},t|r)$ that contributes to $U(k;t|r)$. But for $r < t_1$, the excitation of interest is, in the Eulerian picture, at the low wavenumber p. The connection with wavenumber k comes only through the labeling transforma-

tion that takes place between t_1 and t. Consequently, there is a $\underset{\sim}{k}$ component of $\underset{\sim}{u}(\underset{\sim}{x},t|r)$ that varies with r at the slow rates of evolution of the low wavenumber p, and the contribution of the distortion process to $U(k;t|r)$ decays slowly with r.

The terms in (5.5) which give rise to the tail in R can be seen to describe just this process if the perturbation analysis is traced through in detail. The contribution to $U(k;t|r)$ depends on the shear associated with the low wavenumbers p; unless velocity gradients are present, the modulated displacement of fluid elements cannot generate modulation of the velocity field.

A similar but more involved argument gives the physical basis for the tail on G. The essential point is that, because of differential displacement of fluid elements (labeling transformation), the externally imposed perturbation in the field $\underset{\sim}{u}(\underset{\sim}{x},t|r)$ which produces a pure wavenumber k perturbation in $\underset{\sim}{u}(\underset{\sim}{x},t|t)$ must contain all wavenumbers, including low wavenumbers p which evolve slowly.

According to the LHDI closure formulas, the functions $R(k;t|r)$ and $G(k;t|r)$ determine the effective memory times for the buildup of triple correlations and energy transfer. The action of wavenumbers $<<k$ in making the functions more persistent therefore tends to lengthen these memory times. An interpretation is the following: Production of high wavenumbers involves stretching of large-scale spatial structures into structures having small transverse scales. During this process, the correlations present in the large scales are not destroyed exponentially with repeated halvings of scale size, but tend to persist throughout the straining process. In wavenumber language, the triple correlations associated with energy transfer tend themselves to be transferred up the wavenumber spectrum.

7. LAGRANGIAN AND EULERIAN STRUCTURE FUNCTIONS

A generalized spacetime structure-function tensor may be defined by

$$B_{ij}(\underset{\sim}{x},t|r;\underset{\sim}{x}',t'|r') = \langle[u_i(\underset{\sim}{x},t|r) - u_i(\underset{\sim}{x}',t'|r')] \times [u_j(\underset{\sim}{x},t|r) - u_j(\underset{\sim}{x}',t'|r')]\rangle. \qquad (7.1)$$

The structure tensor measures the velocity difference between two fluid elements. The invariance property

$$\partial U_{ij}(\underset{\sim}{x},t|r;\underset{\sim}{x},t|r')/\partial t = 0 \qquad (7.2)$$

for homogeneous turbulence was obtained in Ref. 1. It expresses that the transformation from Eulerian to Lagrangian coordinates preserves volume in an incompressible fluid.[11] For isotropic turbulence, (7.1) and (7.2) give

$$B_{ij}(\underset{\sim}{x},t|r;\underset{\sim}{x}',t'|r') = \delta_{ij}[U(r) + U(r')] - 2U_{ij}(\underset{\sim}{x},t|r;\underset{\sim}{x}',t'|r'), \qquad (7.3)$$

where $U(r)$ is the mean-square velocity in any direction at time r.

A purely Lagrangian structure tensor, which compares fluid elements labeled simultaneously, is given by $t = t'$, and a purely Eulerian tensor is given by $r = t$, $r' = t'$. The specialized Lagrangian tensor

$$B_{ij}(\underset{\sim}{x}-\underset{\sim}{x}';t|r) \equiv B_{ij}(\underset{\sim}{x},t|t;\underset{\sim}{x}',t|r) \qquad (7.4)$$

can be evaluated for $t \geq r$ from the abridged LHDI equations. This tensor is purely solenoidal, while the full Lagrangian structure tensor is not.

When the turbulence is isotropic and stationary, standard Fourier transformation formulas[12] yield

$$B(\underset{\sim}{y};t|r) = 4\int_0^\infty [1 - \frac{\sin(ky)}{ky} R(k;t|r)]E(k)dk,$$

$$B_{\|}(\underset{\sim}{y};t|r) = 4\int_0^\infty \{\frac{1}{3} - [\frac{\sin(ky)}{(ky)^3} - \frac{\cos(ky)}{(ky)^2}]R(k;t|r)\}E(k)dk, \qquad (7.5)$$

where B and $B_{\|}$ are, respectively, the trace of $B_{ij}(\underset{\sim}{y};t|r)$ and the diagonal component parallel to $\underset{\sim}{y}$, in a coordinate system aligned with $\underset{\sim}{y}$. The diagonal components perpendicular to $\underset{\sim}{y}$ are each given by $B_x = (B - B_{\|})/2$, and the off-diagonal components vanish in this coordinate system.

If the inertial-range forms (5.1) and (5.2) are substituted into (7.5), the result, denoted here by superscript (1), is

$$B^{(1)}(\underset{\sim}{y};t|r) = \varepsilon^{2/3}y^{2/3}F^{(1)}(\varepsilon^{1/3}\tau/y^{2/3}),$$

$$B_{\|}^{(1)}(\underset{\sim}{y};t|r) = \varepsilon^{2/3}y^{2/3}F_{\|}^{(1)}(\varepsilon^{1/3}\tau/y^{2/3}), \quad \tau = t - r, \qquad (7.6)$$

where

$$F^{(1)}(s) = 4C\int_0^\infty [1 - \frac{\sin x}{x} R(x^{2/3}s)]x^{-5/3}dx,$$

$$F_{\|}^{(1)}(s) = 4C\int_0^\infty [\frac{1}{3} - (\frac{\sin x}{x^3} - \frac{\cos x}{x^2})R(x^{2/3}s)]x^{-5/3}dx, \qquad (7.7)$$

and, in particular,

$$F^{(1)}(0) = \frac{9}{5}\Gamma(\frac{1}{3})\,C = 8.52, \qquad F_{\|}^{(1)}(0) = \frac{3}{11}F^{(1)}(0). \qquad (7.7a)$$

The computed value of C is used in (7.7a).

The integrations over x in (7.7) are transformed wavenumber integrations, and they converge at both limits as a consequence of the properties of R established in Secs. 5 and 6. And if y is the reciprocal of a wavenumber within an extensive inertial range, only inertial-range wavenumbers contribute appreciably to the integrals. Nevertheless, (7.6) does not give the inertial-range structure functions correctly. This can be seen from (4.2). If (4.2) is integrated over the energy-containing range, it yields

$$\int_{\substack{\text{energy}\\ \text{range}}} [\partial R(k;t|r)/\partial t]_{t=r} E(k)dk = -\varepsilon/2. \qquad (7.8).$$

Consequently, if $\tau = t-r$ is in the inertial range of time differences, small compared to the characteristic evolution times of the energy-containing wavenumbers,

$$\int_{\substack{\text{energy}\\ \text{range}}} R(k;t|r)E(k)dk = -(t-r)\varepsilon/2. \qquad (7.9)$$

The factor ky in (7.5) can be replaced by unity with negligible error if k is in the energy-containing range and y^{-1} in the inertial range. Hence there is an additional contribution

$$B^{(2)}(\underset{\sim}{y};t|r) = 2(t-r)\varepsilon, \qquad B_{\parallel}^{(2)}(\underset{\sim}{y};t|r) = 2(t-r)\varepsilon/3, \qquad (7.10)$$

so that

$$B(\underset{\sim}{y};t|r) = \varepsilon^{2/3}y^{2/3}F(\varepsilon^{1/3}\tau/y^{2/3}), \quad B_{\parallel}(\underset{\sim}{y};t|r) = \varepsilon^{2/3}y^{2/3}F_{\parallel}(\varepsilon^{1/3}\tau/y^{2/3}),$$
$$\tau = t - r \geq 0, \qquad (7.11)$$

with

$$F(s) = F^{(1)}(s) + 2s, \qquad F_{\parallel}(s) = F_{\parallel}^{(1)}(s) + 2s/3. \qquad (7.12)$$

If $s \sim 1$, the two contributions to $F(s)$ have comparable magnitudes.

There is no corresponding asymptotic contribution from dissipation-range wavenumbers. The total transfer into the dissipation range equals the transfer out of the energy range, but the dissipation-range contribution to (7.5) is suppressed by the trigonometric coefficients if y is in the inertial range and by the small correlation time of $R(k;t|r)$ if $t-r$ is in the inertial range.

A closer look at how the contributions (7.10) arise shows that actually they should not be considered direct effects of the energy-containing eddies.

Equation (7.2) can be Fourier analyzed just like the energy-balance equation. It then describes a similar cascade process: There is a negative contribution $-2\delta_{ij}\varepsilon/3$ to the left-hand side from the energy-containing range, if t-r is small compared to the characteristic times of the energy-containing eddies. This is balanced by a positive contribution at higher wavenumbers. These properties can be established by analysis similar to that which gives (4.2). Note also the discussion of small scales at the end of Sec. 1.

Thus, if (7.1) is Fourier analyzed before (7.2) is used, there are two equal and opposite energy-range contributions which cancel, and (7.10) appears as a contribution at higher wavenumbers, from the cascade process. The formal analysis evidently indicates an ambiguous origin for (7.10), determined by what implicit uses of conservation and invariance properties have been made.

The physical interpretation of (7.10) seems fairly straightforward: On the average, two particles which are separated by $\underset{\sim}{y}$ at a given time t are undergoing a relative acceleration negatively correlated with the velocity difference, the correlation being measured by the slope of $B^{(2)}(\underset{\sim}{y};t|r)$ as a function of r at r = t. This was discussed at the end of Sec. 1. $B^{(1)}(\underset{\sim}{y};t|r)$ has zero slope at r = t and is a contribution from the part of the relative acceleration which is uncorrelated with the relative velocity at time t. The correlation described by $B^{(2)}(\underset{\sim}{y};t|r)$ is due to straining processes established over finite times. If the velocity is multivariate Gaussian at t_0, so that $T(k,t_0)$ vanishes for all k, then there is no initial correlation of relative acceleration, due to pressure forces, with relative velocity.

The abridged LHDI equations of the present paper do not predict

$B(\underset{\sim}{y};t|r)$ for $r > t$. But clearly the negative slope as a function of r cannot persist. Eventually, $B(\underset{\sim}{y};t|r)$ must increase with r. Note that if two particles, known to be separated by $\underset{\sim}{y}$ at t, have reached a new separation $\underset{\sim}{y}'$ at a later time t', their mean-square velocity difference is not given by $B(\underset{\sim}{y}';t'|t')$. These two particles are members of a special subset of all pairs separated by $\underset{\sim}{y}'$ at t', and have special statistics. The present results at $r = t$ thus do not contradict the proposal by C. C. Lin[13] that the simultaneous correlation of relative velocity and relative acceleration be positive and constant at times sufficiently long after release of a particle pair at an inertial-range spatial separation. The structure function which describes the change with time of simultaneous relative velocity is $B_{ii}(\underset{\sim}{x},t|t';\underset{\sim}{x}-\underset{\sim}{y},t|t')$.

Equation (7.11) is inconvenient for finding

$$B(t-r) \equiv B(0;t|r),$$

which gives the mean-square change of velocity of a single fluid element in the interval t-r. For inertial-range values of τ (not for $\tau \to 0$),

$$B(\tau) = \kappa\varepsilon|\tau|, \qquad \kappa = 6C\int_0^\infty [1 - R(s)]s^{-2}ds + 2. \tag{7.13}$$

The second term in κ is obtained from (7.10), and the first term is obtained by using (5.1) and (5.2) in (7.5) with $y = 0$. Equation (7.12) yields

$$F(s) \approx \kappa s \qquad F_{\|}(s) \approx \kappa s/3, \quad s \gg 1. \tag{7.12a}$$

$B(\tau)$ must be even in τ for stationary turbulence, and this fact has been incorporated into (7.13). The linear dependence of $B(\tau)$ on τ in the inertial range was obtained by Inoue[14] by Kolmogorovian dimensional analysis.

The computed results for $F(s)$ and $F_{\|}(s)$ are plotted in Fig. 4. The

value computed for the integral in (7.13) is 1.46, yielding $\kappa = 17.5$.

The above formulas for the inertial-range Lagrangian structure functions assume stationary isotropic turbulence, which must be maintained by statistically stationary driving forces of some kind. The results are unchanged if the turbulence is freely decaying. This can be verified by retracing the analysis carefully for the freely decaying case. It also can be seen by a simple argument: The decay of the total kinetic energy is given by $\partial u^2/\partial t = -2\varepsilon$, where u is the total rms velocity. The characteristic decay time of u is therefore u^2/ε. In a time $\tau << u^2/\varepsilon$, the mean-square change of velocity due to decay (i.e., due to the lack of energy-range sustaining forces) is $\langle(\Delta u)^2\rangle \sim (\varepsilon\tau/u)^2 \sim \varepsilon\tau[\tau/(u^2/\varepsilon)]$, which is asymptotically negligible compared to the mean-square velocity differences of order $\varepsilon\tau$ found above. Note that mean-square change of velocity does not mean change of mean-square velocity.

A purely Eulerian structure tensor is obtained by setting $r = t$, $r' = t'$ in (7.1). For $t - t'$ small enough that the time dependence of $E(k,t)$ is negligible, the formulas for the Eulerian scalars $B^E(\underset{\sim}{y};t,t')$ and $B_\parallel^E(\underset{\sim}{y};t,t')$, analogous to B and $B_\parallel$, are identical with (7.5), except that $R(k;t|r)$ is replaced by the Eulerian modal correlation function

$$R^E(k;t,t') = 2\pi k^2 U(k;t|t;t'|t')/[E(k,t)E(k,t')]^{1/2}. \qquad (7.14)$$

The Lagrangian and Eulerian modal time correlations measure quite different properties when k is in the inertial range. The Lagrangian correlation is determined by intrinsic distortions of the small-scale structures, and the correlation time is of order $(v_k k)^{-1}$, where v_k is the rms velocity in wavenumbers $\geq k$. The Eulerian correlation is dominated by the convection

of the small scales by the energy-containing scales.

The convection of a frozen small-scale structure by a uniform velocity $\underset{\sim}{u}$ induces the time dependence $\exp(-i\underset{\sim}{k}\cdot\underset{\sim}{u})$ in the Fourier amplitude $\underset{\sim}{k}$ of the small-scale structure. Now assume, in accord with Kolmogorov's hypotheses, that the distribution of the small-scale velocity fluctuations is statistically independent of the simultaneously measured distribution of the convecting velocity. Then it follows immediately that

$$R^E(\underset{\sim}{k};t,t-\tau) = M(\underset{\sim}{k}\tau,t), \tag{7.15}$$

where

$$M(\underset{\sim}{\alpha},t) = \left\langle e^{-i\underset{\sim}{\alpha}\cdot\underset{\sim}{u}} \right\rangle = \int e^{-i\underset{\sim}{\alpha}\cdot\underset{\sim}{u}} P(\underset{\sim}{u},t)d^3u \tag{7.16}$$

is the characteristic function of the one-point probability distribution $P(\underset{\sim}{u},t)$ of the convecting velocity at time t. The correlation time indicated by (7.15) is $(v_0k)^{-1}$, where v_0 is the rms value of any vector component of the convecting velocity, now identified with the energy-range velocity. Since this correlation time is $<< (v_kk)^{-1}$, it may be concluded that distortion effects make a negligible change in the Eulerian time correlation and that (7.15) is the complete asymptotic result for inertial-range k. Finally, $P(\underset{\sim}{u},t)$ in (7.16) may be taken as the one-point distribution of the entire velocity, since the energy-range contributions dominate the latter distribution.

Equation (7.15) follows also for dissipation-range wavenumbers if the relevant distortion time for scales of order k^{-1} is assumed to be not less than the Kolmogorov time $(\nu/\varepsilon)^{1/2}$ regardless of how high k may be. In other words, it is necessary that the very small-scale structures follow the structures of scale k_s^{-1} and not exhibit independent distortions.

The result for the Eulerian modal response function $G^E(\underset{\sim}{k};t,t')$ corresponding to (7.15) is

$$G^E(\underset{\sim}{k};t,t-\tau) = \exp(-\nu k^2\tau)M(\underset{\sim}{k}\tau,t), \tag{7.17}$$

for $\underset{\sim}{k}$ in the inertial or dissipation range. The viscous factor appears in (7.17) because an arbitrary perturbation at a wavenumber high in the dissipation range will be uncorrelated with the existing structures, will not be supported by them, and will decay, during the convection by energy-range scales, as if in isolation. Note that $\nu k_s^2 << v_0 k_s$, so that when the inertial range is extensive the viscous damping in (7.17) is negligible except for k in the far dissipation range.

Equations (7.15) and (7.17) are presumably exact results if the underlying assumption of asymptotic statistical independence of simultaneously measured small- and large-scale structures is valid. No closure approximation is used, and isotropy of the energy-containing range is not invoked.

The abridged LHDI equations do not predict Eulerian time correlations. However, the unabridged LHDI approximation leads easily to explicit results for $R^E(\underset{\sim}{k};t,t')$ and $G^E(\underset{\sim}{k};t,t')$ when $\underset{\sim}{k}$ is high enough that $(v_0 k)^{-1}$ is short compared to Lagrangian correlation times for mode $\underset{\sim}{k}$. In that case, the Galilean invariance properties of the LHDI equations[1] imply directly that

$$\begin{aligned} R^E(k;t,t-\tau) &= \exp[-\tfrac{1}{2} v_0^2 k^2 \tau^2], \\ G^E(k;t,t-\tau) &= \exp[-\nu k^2\tau - \tfrac{1}{2} v_0^2 k^2 \tau^2], \end{aligned} \tag{7.18}$$

in the isotropic case. This agrees with (7.15) and (7.17) if the univariate velocity distribution is Gaussian. Thus the accuracy of the LHDI results depends on how close the actual univariate distribution is to Gaussian.

In the case of inhomogeneous turbulence with nonzero mean velocity, the LHDI result again is exact if and only if the univariate velocity distribution is normal.

Insertion of (7.18) into the formulas for B^E and $B_{\|}^E$ yields

$$B^E(\underset{\sim}{y};t,t') = \epsilon^{2/3}y^{2/3}F^E(v_0\tau/y), \quad B_{\|}^E(\underset{\sim}{y};t,t') = \epsilon^{2/3}y^{2/3}F_{\|}^E(v_0\tau/y),$$

$$\tau = t - t', \tag{7.19}$$

where

$$F^E(s) = 4C\int_0^\infty [1 - \frac{\sin x}{x}\exp(-\tfrac{1}{2}x^2s^2)]x^{-5/3}dx,$$

$$F_{\|}^E(s) = 4C\int_0^\infty [\frac{1}{3} - (\frac{\sin x}{x^3} - \frac{\cos x}{x^2})\exp(-\tfrac{1}{2}x^2s^2)]x^{-5/3}dx. \tag{7.20}$$

Also,

$$B^E(\tau) = \kappa^e(\epsilon v_0\tau)^{2/3}, \quad \kappa^e = 4C\int_0^\infty [1 - \exp(-\tfrac{1}{2}s^2)]s^{-5/3}ds, \tag{7.21}$$

where $B^E(t-t') \equiv B^E(0;t,t')$. Equation (7.21) gives the mean-square velocity change at a fixed point in laboratory coordinates. Equations (7.19)-(7.21) are valid for y and $v_0\tau$ in the inertial range of spatial scales. There are no contributions analogous to (7.10); $R^E(k;t,t')$ has zero slope at $t = t'$ for all wavenumbers, in stationary turbulence.

$F^E(s)$ and $F_{\|}^E(s)$ are plotted in Fig. 5. The integral in (7.21) has the value 1.61, yielding $\kappa^e = 11.4$. Equation (7.20) yields

$$F^E(s) \approx \kappa^e s^{2/3}, \quad F_{\|}^E(s) \approx \kappa^e s^{2/3}/3, \quad s >> 1. \tag{7.20a}$$

8. LAGRANGIAN ACCELERATION AND PRESSURE COVARIANCES

The function

$$\underset{\sim}{a}(\underset{\sim}{x},t|r) = \partial \underset{\sim}{u}(\underset{\sim}{x},t|r)/\partial r \tag{8.1}$$

is the acceleration at time r of the fluid element which arrives at $\underset{\sim}{x}$ at time t. The two simplest Lagrangian covariances between acceleration and velocity are

$$K_{ij}(\underset{\sim}{y};t|r) = \left\langle u_i(\underset{\sim}{x},t|t)a_j(\underset{\sim}{x}-\underset{\sim}{y},t|r)\right\rangle \tag{8.2}$$

and

$$K^{\dagger}_{ij}(\underset{\sim}{y};t|r) = \left\langle u_i(\underset{\sim}{x},t|r)a_j(\underset{\sim}{x}-\underset{\sim}{y},t|t)\right\rangle. \tag{8.3}$$

Given a pair of particles known to be separated by $\underset{\sim}{y}$ at time t, K_{ij} measures the correlation between the velocity of one at time t and the acceleration of the other at a time r. $K^{\dagger}_{ij}$ measures the correlation between the velocity of the first at time r and the acceleration of the second at time t.

The relation between K_{ij} and $K^{\dagger}_{ij}$ is simplest in stationary, homogeneous turbulence. To permit such turbulence, let a stationary, homogeneous, solenoidal forcing field $\underset{\sim}{f}(\underset{\sim}{x},t)$ be introduced so that the Navier-Stokes equation is

$$[\partial/\partial t + \underset{\sim}{u}(\underset{\sim}{x},t|t)\cdot\underset{\sim}{\nabla}]\underset{\sim}{u}(\underset{\sim}{x},t|t) = \underset{\sim}{a}(\underset{\sim}{x},t|t), \tag{8.4}$$

$$\underset{\sim}{a}(\underset{\sim}{x},t|t) = \nu\nabla^2\underset{\sim}{u}(\underset{\sim}{x},t|t) - \underset{\sim}{\nabla}p(\underset{\sim}{x},t) + \underset{\sim}{f}(\underset{\sim}{x},t), \tag{8.5}$$

where $p(\underset{\sim}{x},t)$ is the kinematic pressure field. The nature of $\underset{\sim}{f}(\underset{\sim}{x},t)$ need not be specified further. The forces may, but need not, be negative dampings as in Sec. 4. In the stationary state,

$$K_{ij}(\underset{\sim}{x}-\underset{\sim}{x}';t|r) = \partial U_{ij}(\underset{\sim}{x},t|t;\underset{\sim}{x}',t|r)/\partial r = -\partial U_{ij}(\underset{\sim}{x},t|t;\underset{\sim}{x}',t|r)/\partial t. \tag{8.6}$$

An expression for the last member of (8.6) is readily obtained by multiplying (8.4) with $\underset{\sim}{u}(\underset{\sim}{x}',t|r)$, multiplying (1.2) with $\underset{\sim}{u}(\underset{\sim}{x},t|t)$, adding, and averaging. This gives

$$K_{ij}(\underset{\sim}{x}-\underset{\sim}{x}';t|r) = \left\langle u_j(\underset{\sim}{x}',t|r)u_n(\underset{\sim}{x},t|t)\partial u_i(\underset{\sim}{x},t|t)/\partial x_n\right\rangle$$

$$+ \left\langle u_i(\underset{\sim}{x},t|t)u_n(\underset{\sim}{x}',t|t)\partial u_j(\underset{\sim}{x}',t|r)/\partial x_n'\right\rangle - \left\langle u_j(\underset{\sim}{x}',t|r)a_i(\underset{\sim}{x},t|t)\right\rangle. \quad (8.7)$$

If the second term on the right-hand side is rewritten using $\partial u_n(\underset{\sim}{x}',t|t)/\partial x_n' = 0$ and homogeneity, (8.7) becomes

$$K_{ij}(\underset{\sim}{x}-\underset{\sim}{x}';t|r) = - K_{ji}^{\dagger}(\underset{\sim}{x}'-\underset{\sim}{x};t|r)$$

$$+ \left\langle u_j(\underset{\sim}{x}',t|r)[u_n(\underset{\sim}{x},t|t) - u_n(\underset{\sim}{x}',t|t)]\partial u_i(\underset{\sim}{x},t|t)/\partial x_n\right\rangle. \quad (8.8)$$

Equation (8.8) shows that $K_{ij}(\underset{\sim}{x}-\underset{\sim}{x}';t|r) = - K_{ji}^{\dagger}(\underset{\sim}{x}'-\underset{\sim}{x};t|r)$ if $\underset{\sim}{x} = \underset{\sim}{x}'$, but not if $\underset{\sim}{x} \neq \underset{\sim}{x}'$. The result for $\underset{\sim}{x} = \underset{\sim}{x}'$ can also be obtained from differentiation of

$$U_{ij}(\underset{\sim}{x},t|t;\underset{\sim}{x},t|r) = U_{ij}(\underset{\sim}{x},r|t;\underset{\sim}{x},r|r), \quad (8.9)$$

a relation which follows from (7.2). Moreover, the evenness of $U_{ii}(\underset{\sim}{x},t|t;\underset{\sim}{x},t|r)$ in t-r shows that $K(t-r) \equiv K_{ii}(0;t|r)$ is an odd function of t-r.

K_{ij} is solenoidal in i because the Eulerian velocity is solenoidal, and is solenoidal in j also if the turbulence is homogeneous and reflection-invariant. In the stationary state,

$$- \partial U_{ij}(\underset{\sim}{x},t|t;\underset{\sim}{x}',t|r)/\partial t = \frac{1}{2}\,\partial B_{ij}(\underset{\sim}{x},t|t;\underset{\sim}{x}',t|r)/\partial t, \quad (8.10)$$

so that for stationary, isotropic turbulence (7.11) yields

$$K(\underset{\sim}{y};t|r) = \frac{1}{2}\,\varepsilon\dot{F}(\varepsilon^{1/3}\tau/y^{2/3}), \qquad K_{\|}(\underset{\sim}{y};t|r) = \frac{1}{2}\,\varepsilon\dot{F}_{\|}(\varepsilon^{1/3}\tau/y^{2/3}),$$

$$\tau = t - r \geq 0 \qquad \text{(stationary turbulence)}, \quad (8.11)$$

where K and $K_{\parallel}$ are the trace and the longitudinal, diagonal element of K_{ij}. The functions

$$\dot{F}(s) = dF(s)/ds, \quad \dot{F}_{\parallel}(s) = dF_{\parallel}(s)/ds$$

are plotted in Fig. 6. Equation (7.13) yields

$$K(\tau) = \frac{1}{2} \kappa\varepsilon \text{ sgn } \tau \qquad \text{(stationary turbulence).} \qquad (8.12)$$

It must be remembered that (8.12) is established only for $|\tau|$ in the inertial range of times and is invalid for $|\tau| \to 0$.

The change of sign in (8.12) has a simple physical interpretation. For $\tau > 0$, $K(\tau)$ measures the correlation of a particle's velocity with its previous acceleration. This is positive because the velocity increment produced by the acceleration shows some persistence. On the other hand, a negative correlation of velocity with later acceleration is necessary if the velocity is to change direction without increasing its magnitude, in mean square. Contrast this behavior of one-particle velocity and acceleration with the opposite correlation of relative velocity and relative acceleration of two particles, as indicated by the slope of $B(\underset{\sim}{y},t|r)$ at $r = t$ [Equations (7.10) and (7.11), et seq.].

A constant negative value of $K(\tau)$ for τ negative and in the inertial range has been proposed on the basis of a kind of Brownian-motion model of the behavior in velocity space.[15,16] The present result does not seem properly explicable in terms of such a model. The major contribution to $K(\tau)$ at an inertial-range τ comes from eddies whose circulation times are of order τ. A Brownian-motion model requires that instead the major effect come from eddies whose circulation times are $\ll \tau$, so that many uncorrelated eddies contribute. The similarity of the results of the two

approaches seems fortuitous, but this may be a premature conclusion.

Conservation of energy requires

$$\left\langle u_i(\underset{\sim}{x},t|t)f_j(\underset{\sim}{x},t|t)\right\rangle = \frac{1}{3}\,\delta_{ij}\varepsilon \tag{8.13}$$

in stationary, isotropic turbulence. If the driving forces f_j are confined to the energy-containing range, then (8.13) is nearly satisfied with $u_i(\underset{\sim}{x},t|t)$ replaced by $u_i(\underset{\sim}{x}',t|r)$, provided that $|\underset{\sim}{x}-\underset{\sim}{x}'|$ and t-r are small compared to energgy-range space and time scales. In this case, (8.5) yields

$$K^{\dagger}_{ij}(\underset{\sim}{x}-\underset{\sim}{x}';t|r) = \nu\nabla^2_{x'}U_{ij}(\underset{\sim}{x},t|r;\underset{\sim}{x}',t|t) + D_{ij}(\underset{\sim}{x}-\underset{\sim}{x}';t|r) + \frac{1}{3}\,\delta_{ij}\varepsilon, \tag{8.14}$$

where

$$D_{ij}(\underset{\sim}{x}-\underset{\sim}{x}';t|r) = -\left\langle u_i(\underset{\sim}{x},t|r)\partial p(\underset{\sim}{x}',t)/\partial x'_j\right\rangle \tag{8.15}$$

is the covariance of pressure gradient with Lagrangian velocity. D_{ij} is a pure antisolenoidal tensor in homogeneous, reflection-invariant turbulence. Its curl with respect to each index vanishes.

The right-hand side of (8.15) can be converted into a third-order moment of the velocity field by eliminating the pressure in standard fashion. The triple moment can be evaluated for $t \geq r$ by the abridged LHDI approximation of Ref. 1. The result for isotropic turbulence is

$$D(\underset{\sim}{y};t|r) = \int_0^\infty \tilde{Q}(k;t|r)\frac{\sin(ky)}{ky}\,dk,$$

$$D_x(\underset{\sim}{y};t|r) = \int_0^\infty \tilde{Q}(k;t|r)\left[\frac{\sin(ky)}{(ky)^3} - \frac{\cos(ky)}{(ky)^2}\right]dk, \tag{8.16}$$

where

$$\tilde{Q}(k;t|r) = -4\pi^2k^2\iint_\Delta dpdq\; p^2qh_{kpq}U(p;t|r)\int_r^t U(q;t|s)ds,$$

$$h_{kpq} = (1-z^2)(z+xy). \tag{8.17}$$

In (8.16), D and D_x are the trace and diagonal element perpendicular to $\underset{\sim}{y}$. The diagonal element parallel to $\underset{\sim}{y}$ is given by $D_{\|} = D - 2D_x$, and the off-diagonal elements vanish in a coordinate system aligned with $\underset{\sim}{y}$. In (8.17), x, y, and z are the cosines of the interior angles opposite k, p, and q in a triangle with these wavenumbers as sides.

For $|\underset{\sim}{x}-\underset{\sim}{x}'|$ and/or t-r in the inertial range of separations, assume that the ν term in (8.14) is negligible, subject to later check. Then $K^{\dagger}_{ij}$ is purely curlfree, in contrast to K_{ij} which is purely solenoidal. If the inertial-range forms (5.1) and (5.2) are substituted into (8.17), the result can be written

$$\tilde{Q}(k;t|t-\tau) = -C^2\varepsilon k^{-1}Q(\varepsilon^{1/3}k^{2/3}\tau), \tag{8.18}$$

where

$$Q(s) = \int_0^\infty du \int_{|u-1|}^{u+1} dv\, h_{luv} u^{-5/3} v^{-8/3} R(u^{2/3}s) \int_0^s R(v^{2/3}w)dw. \tag{8.19}$$

The function Q(s) is plotted in Fig. 7. For $s \gg 1$, $Q(s) \sim s^{-2}$, to within a factor that varies more slowly than any power of s. Equation (8.18) gives

$$D(\underset{\sim}{y};t|r) = -\varepsilon Z(\varepsilon^{1/3}\tau/y^{2/3}), \quad D_x(\underset{\sim}{y};t|r) = -\varepsilon Z_x(\varepsilon^{1/3}\tau/y^{2/3}),$$
$$\tau = t - r, \tag{8.20}$$

with

$$Z(s) = C^2 \int_0^\infty \frac{\sin x}{x} Q(x^{2/3}s)\frac{dx}{x},$$

$$Z_x(s) = C^2 \int_0^\infty \left[\frac{\sin x}{x^3} - \frac{\cos x}{x^2}\right] Q(x^{2/3}s)\frac{dx}{x}. \tag{8.21}$$

Also,

$$D(0;t|r) = -\frac{3}{2} C^2 \varepsilon \int_0^\infty Q(s)\frac{ds}{s}. \tag{8.22}$$

Using these values for the pressure contribution to $K^{\dagger}_{ij}$ in the inertial range, it can be verified that the viscous contribution to (8.14) is negligible in comparison if t-r is large compared to the Kolmogorov time $(\nu/\varepsilon)^{1/2}$. The check consists of assuming a long inertial range and evaluating the total viscous contribution from the whole range of wavenumbers up to $k_s = (\varepsilon/\nu^3)^{1/4}$, using the forms (5.1) and (5.2) and using the properties of $R(\tau)$ for long τ discussed in Sec. 6.

The final inertial-range results are

$$K^{\dagger}(\underset{\sim}{y};t|r) = -\varepsilon Z(\varepsilon^{1/3}\tau/y^{2/3}) + \varepsilon, \quad K^{\dagger}_{x}(\underset{\sim}{y};t|r) = -\varepsilon Z_{x}(\varepsilon^{1/3}\tau/y^{2/3}) + \varepsilon/3,$$

$$\text{(stationary turbulence)} \qquad \tau = t - r, \tag{8.23}$$

$$K^{\dagger}(\tau) = -\frac{3}{2}C^2\varepsilon\int_0^{\infty} Q(s)\frac{ds}{s} + \varepsilon \quad \text{(stationary turbulence)}, \tag{8.24}$$

where $K^{\dagger}(\underset{\sim}{y};t|r)$ and $K^{\dagger}_{x}(\underset{\sim}{y};t|r)$ are the trace and transverse diagonal element of $K^{\dagger}_{ij}(\underset{\sim}{y};t|r)$, and $K^{\dagger}(t-r) \equiv K^{\dagger}(0;t|r)$. The functions $Z(s)$ and $Z_x(s)$ are plotted in Fig. 8. The computed value of the right-hand side of (8.24) is $-8.96\,\varepsilon$. Equation (8.23) yields

$$K^{\dagger}(\underset{\sim}{y};t|t-\tau) \approx K^{\dagger}(\tau), \quad K^{\dagger}_{x}(\underset{\sim}{y};t|t-\tau) \approx \frac{1}{3}K^{\dagger}(\tau), \quad \varepsilon^{1/3}\tau/y^{2/3} \gg 1. \tag{8.23a}$$

According to (8.8),

$$K(\tau) = -K^{\dagger}(\tau). \tag{8.25}$$

Thus if (7.13), (8.12), and (8.24) are consistent equations, C and R(s) must satisfy

$$3C\int_0^{\infty}[1 - R(s)]s^{-2}ds + 1 = \frac{3}{2}C^2\int_0^{\infty}Q(s)\frac{ds}{s} - 1, \tag{8.26}$$

with Q(s) given by (8.19). This consistency is assured by the abridged

LHDI procedure. The calculation of K_{ij} by (8.6) amounts to evaluating the right-hand side of (8.7), using the abridged LHDI recipe for all the triple moments. The vanishing of the last term on the right-hand side of (8.8) at $\underset{\sim}{x} = \underset{\sim}{x}'$ survives the approximation because $u_n(\underset{\sim}{x},t|t)$ and $u_n(\underset{\sim}{x}',t|t)$ receive similar treatments. Equation (8.26) is a useful overall check on the algebra and numerical calculations (see Appendix).

The Lagrangian acceleration covariance

$$A_{ij}(\underset{\sim}{x}-\underset{\sim}{x}';t|r) = \langle a_i(\underset{\sim}{x},t|r)a_j(\underset{\sim}{x}',t|t)\rangle \tag{8.27}$$

can be evaluated by using the relation

$$A_{ij}(\underset{\sim}{x}-\underset{\sim}{x}';t|r) = \partial K^{\dagger}_{ij}(\underset{\sim}{x}-\underset{\sim}{x}';t|r)/\partial r. \tag{8.28}$$

This yields the inertial-range results

$$A(\underset{\sim}{y};t|t-\tau) = \varepsilon^{4/3}y^{-2/3}\dot{Z}(\varepsilon^{1/3}\tau/y^{2/3}), \quad A_x(y;t|t-\tau) = \varepsilon^{4/3}y^{-2/3}\dot{Z}_x(\varepsilon^{1/3}\tau/y^{2/3}) \tag{8.29}$$

where A and A_x are the trace and transverse diagonal element of A_{ij}. The functions

$$\dot{Z}(s) = dZ(s)/ds, \quad \dot{Z}_x(s) = dZ_x(s)/ds$$

are plotted in Fig. 9. The quantity $dQ(s)/ds$ determined by (8.19) can be evaluated analytically at $s = 0$ [see (8.36), (8.37)], when

$$\dot{Z}(0) = \frac{14}{121}\left[\frac{9}{5}\Gamma(\tfrac{1}{3})\right]^2 C^2 = 8.39, \qquad \dot{Z}_x(0) = \frac{3}{7}\dot{Z}(0). \tag{8.30}$$

The covariance of acceleration along a particle trajectory is $A(t-r) \equiv A(0;t|r)$. It satisfies

$$A(\tau) = -\,dK^{\dagger}(\tau)/d\tau. \tag{8.31}$$

Differentiation of (8.24) with respect to τ gives zero. This says that

there is no inertial-range contribution to $A(\tau)$ proportional to $\varepsilon\tau^{-1}$, the form that might be suggested by Kolmogorov scaling. For given τ, the positive contributions to $A(\tau)$ from some inertial-range wavenumbers are balanced by negative contributions from other wavenumbers. A relevant fact is that the pressure forces conserve energy and cannot change the mean-square particle velocity. If there were a nonzero net inertial-range contribution of the form $\varepsilon\tau^{-1}$, then the inertial range (where only pressure forces cause acceleration) would give a nonzero contribution to $\int_0^\infty A(s)ds$, the total rate of change of kinetic energy. Also, a contribution of the form $\varepsilon\tau^{-1}$ to $A(\tau)$ would imply a contribution of form $-\varepsilon \ln(\varepsilon^{1/2}\tau/\nu^{1/2})$ to $K^\dagger(\tau)$, which would violate Kolmogorov's concept of a ν-independent inertial range.

In contrast to the results for the structure functions, the inertial-range formulas for K_{ij} and $K^\dagger_{ij}$ are altered if the turbulence is freely decaying instead of stationary. The free-decay results are obtained simply by subtracting off the driving term in (8.14), seq. Thus (8.11), (8.12), (8.14), (8.23)-(8.25) are replaced by

$$\underset{\sim}{K}(\underset{\sim}{y};t|r) = \tfrac{1}{2}\varepsilon\dot{F}(\varepsilon^{1/3}\tau/y^{2/3}) - \varepsilon,$$

$$K_{\parallel}(\underset{\sim}{y};t|r) = \tfrac{1}{2}\varepsilon\dot{F}_{\parallel}(\varepsilon^{1/3}\tau/y^{2/3}) - \varepsilon/3, \tag{8.11'}$$

$$K(\tau) = \varepsilon(-1 + \tfrac{1}{2}\kappa \operatorname{sgn}\tau), \tag{8.12}$$

$$K^\dagger_{ij}(\underset{\sim}{x}-\underset{\sim}{x}';t|r) = \nu\nabla^2_{x'}U_{ij}(\underset{\sim}{x},t|r;\underset{\sim}{x}',t|t) + D_{ij}(\underset{\sim}{x}-\underset{\sim}{x}';t|r), \tag{8.14'}$$

$$K^\dagger(\underset{\sim}{y};t|t-\tau) = -\varepsilon Z(\varepsilon^{1/3}\tau/y^{2/3}), \quad K^\dagger_x(\underset{\sim}{y};t|t-\tau) = -\varepsilon Z_x(\varepsilon^{1/3}\tau/y^{2/3}), \tag{8.23'}$$

$$K^{\dagger}(\tau) = -\frac{3}{2} C^2 \varepsilon \int_0^{\infty} Q(s) \frac{ds}{s} , \tag{8.24'}$$

$$K(\tau) + 2\varepsilon = -K^{\dagger}(\tau), \tag{8.25'}$$

where a corresponding subtraction of the driving-force contribution has been made from (8.11) and (8.12). These changes express that the decay of the turbulence requires a deceleration of the particles, on the average. By conservation of energy, the deceleration must contribute $-\varepsilon$ to $K(0)$, an amount which is comparable to the inertial-range contributions and superposed upon them. Equations (8.18) - (8.22) and (8.29)-(8.31) are unchanged. The contribution of the decay deceleration to A_{ij} is of order ε^2/v_0^2, where v_0 is the total rms velocity component. This is smaller than the inertial-range contributions (8.29) by a factor of order $(y/\ell_0)^{2/3}$, where ℓ_0 is the characteristic energy-range spatial scale, and therefore does not appear in the asymptotic formulas.

It is a matter of taste whether the overall deceleration in decaying turbulence should be considered an energy-range effect. Actually, all scales of motion are involved: The loss of kinetic energy occurs at dissipation-range scales, in the Eulerian picture, so that the entire cascade plays a role. It is clear, however, that the scales of order y play no special role in determining the deceleration contribution to $K(\underset{\sim}{y};t|r)$ when y is an inertial-range separation. Therefore it seems justified to consider the steady-state formulas as the "true" inertial-range expressions.

The functions discussed above give some limited information about pressure statistics. By (8.1) and (8.15),

$$[\partial D_{ij}(\underset{\sim}{x}-\underset{\sim}{x}';t|r)/\partial r]_{r=t} = -\left\langle a_i(\underset{\sim}{x},t|r)\partial p(\underset{\sim}{x}',t)/\partial x_j'\right\rangle . \tag{8.32}$$

In homogeneous, reflection-invariant turbulence, only the curlfree term $-\underset{\sim}{\nabla}p$ in (8.5) can contribute to (8.32). Hence,

$$\left\langle[\partial p(\underset{\sim}{x},t)/\partial x_i][\partial p(\underset{\sim}{x}',t)/\partial x_j']\right\rangle = [\partial D_{ij}(\underset{\sim}{x}-\underset{\sim}{x}';t|r)/\partial r]_{r=t} . \tag{8.33}$$

The pressure spectrum function [satisfying mean-square-pressure $= \int_0^\infty P(k,t)dk$] is therefore

$$P(k,t) = k^{-2}[\partial\tilde{Q}(k;t|r)/\partial r]_{r=t} \tag{8.34}$$

in isotropic turbulence. By (8.17), this gives

$$P(k,t) = \iint_\Delta dpdq\ p^2qh_{kpq}E(p,t)E(q,t). \tag{8.35}$$

This abridged LHDI result for P(k,t) is identical, after trigonometric manipulations, with the quasinormality approximation for P(k,t) used by Heisenberg[3] and Batchelor.[12] The unabridged LHDI expression for P(k,t) does not appear to reduce to the quasinormality approximation.

In the inertial range, (8.35) yields

$$P(k,t) = C^2\varepsilon^{4/3}k^{-7/3}\int_0^\infty du\int_{|u-1|}^{u+1} dv\ h_{luv}u^{-5/3}v^{-8/3}. \tag{8.36}$$

Using trigonometric identities and results of Oboukhov,[17] the quadratures can be performed to give

$$P(k,t) = \frac{70\sqrt{3}}{121\pi}\left[\frac{3}{5}\Gamma(\tfrac{1}{3})\right]^3C^2\varepsilon^{4/3}k^{-7/3} = 4.13\ \varepsilon^{4/3}k^{-7/3}, \tag{8.37}$$

and

$$\left\langle[p(\underset{\sim}{x},t - p(\underset{\sim}{x}+\underset{\sim}{y},t)]^2\right\rangle = [B_{\|}(\underset{\sim}{y};t|t)]^2 = 5.39\ \varepsilon^{4/3}y^{4/3}. \tag{8.38}$$

A Lagrangian pressure field $p(\underset{\sim}{x},t|r)$ can be defined as the pressure

at time r in the fluid element which arrives at $\underset{\sim}{x}$ at time t. The contribution $\underset{\sim}{\alpha}(\underset{\sim}{x},t|r)$ of the pressure field to $\underset{\sim}{a}(\underset{\sim}{x},t|r)$ is the negative of the pressure gradient in the fluid element at time r. Except in degenerate cases,

$$\underset{\sim}{\alpha}(\underset{\sim}{x},t|r) \neq -\underset{\sim}{\nabla}p(\underset{\sim}{x},t|r) \qquad (t \neq r), \tag{8.39}$$

because $\underset{\sim}{x}$ is a Lagrangian coordinate at time r, not a laboratory Cartesian coordinate. Consequently, the Lagrangian spacetime structure function $\langle[p(\underset{\sim}{x},t) - p(\underset{\sim}{x}',t|r)]^2\rangle$ is not obtained by simply extending (8.33)-(8.38) to $r \neq t$.

9. COMPARISON OF INERTIAL-RANGE PREDICTIONS WITH EXPERIMENT

The qualitative inertial-range predictions of the abridged LHDI equations are implied by Kolmogorov's hypotheses and the associated dimensional analysis. Experimental testing of the results therefore involves, first of all, a test of the Kolmogorov theory. The Kolmogorov scaling laws have received support from measurements of energy spectra at high Reynolds numbers, and such measurements appear to offer the principal check available on quantitative predictions of inertial- and dissipation-range properties.

The Kolmogorov constant is customarily estimated from experiment by choosing, visually, best-fitting straight lines to log-log plots of spectrum versus wavenumber. The normalization parameter ε is determined by drawing a best-looking curve through a plot of the dissipation spectrum, and using isotropic relations. The fitting of a best straight line requires an explicit or implicit estimate of the maximum wavenumber at which dissipation

effects on spectrum shape can be neglected in comparison with experimental scatter. This estimate plays a significant role because, as the Figures to follow illustrate, the experiments cover very limited inertial ranges. Consequently, it is desirable to compare the data directly with predictions of the entire Kolmogorov spectrum, instead of merely comparing the experimental and theoretical estimates of the Kolmogorov constant.

The abridged LHDI prediction of the Kolmogorov spectrum in the dissipation range has been obtained by taking $U(k;t_0|t_0) \propto k^{-11/3}$ over a wide k range, and then integrating (2.6)-(2.8) forward in time, with nonzero viscosity. The calculation was continued until the normalized dissipation spectrum $(k/k_s)^2E(k)/(\varepsilon^{1/4}\nu^{5/4})$ reached and held steady-state values. Further details of the calculation are given in the Appendix. One-dimensional spectra were then computed from the formulas

$$\phi_1(k) = \frac{1}{2}\int_k^\infty E(p)(1 - k^2/p^2)p^{-1}dp, \quad \phi_{tot}(k) = \int_k^\infty E(p)p^{-1}dp. \tag{9.1}$$

Here $\phi_1(k)$ is the longitudinal one-dimensional spectrum[12] and $\phi_{tot}(k)$ is the sum of the longitudinal and the two transverse spectrum functions. The corresponding asymptotic inertial-range spectra are

$$\phi_1(k) = (9/55)C\varepsilon^{2/3}k^{-5/3}, \qquad \phi_{tot}(k) = (3/5)C\varepsilon^{2/3}k^{-5/3}. \tag{9.2}$$

The computed values of $(k/k_s)^{5/3}\phi_1(k)/(\varepsilon^{1/4}\nu^{5/4})$ from the inertial and dissipation-range calculations are plotted together in Fig.10. This kind of plot displays differences in inertial-range spectra more prominently than the usual log-log spectrum plot. Note that the low-wavenumber end of the decay-calculation curve rises slightly above the asymptotic inertial-range line C = 1.77. This is due to truncation of the wavenumber range and to

the finite time of evolution, each of which tends to depress ε below its asymptotic value. A more precise computation would yield a curve lying slightly below that shown, in the range $.002 < (k/k_s) < .02$.

The experimental points plotted in Fig. 10 are sea-water data obtained by Grant, Stewart, and Moilliet.[18] These experiments appear to be the highest-Reynolds-number measurements of absolute spectrum levels which have been reported ($R_\lambda \sim 3000$). The points represent the three runs on 3 October 1959. The run at 0950 hrs was cited as particularly satisfactory with regard to scatter and noise level; it is plotted in different ways in Figs. 8-10 of Ref. 18. The dissipation spectra $(k/k_s)^2\phi_1(k)/(\varepsilon^{1/4}\nu^{5/4})$ for the three runs are displayed in a linear plot in Fig. 11, together with the theoretical curve. Both data and theory indicate a maximum at about $(k/k_s) = 0.09$. At this value of k/k_s, the curve in Fig. 10 is down from the asymptotic inertial-range line by about 30%.

Figure 10 illustrates the difficulties in accurate experimental determination of C. Only eight points lie in the range $(k/k_s) < .01$, where the theoretical curve indicates negligible deviation from the asymptotic inertial-range level. These eight points scatter from 20% below to 25% above the computed inertial-range line. The 17 runs reported in Ref. 18 show substantially greater scatter at $(k/k_s) < .01$ than in the dissipation range $.01 < (k/k_s) < .5$, both individually and collectively. The fluctuations at low k seem oscillatory rather than random, possibly as a result of coupling between the turbulence and the towed body on which the sensors were mounted.[18] Figure 12 compares the three longest runs on 1 February 1960, and on 2 February 1960, with the theoretical curve. The

oscillations are particularly prominent in the run at 1331 hrs on 1 February.

Grant, Stewart, and Moilliet report a mean determination C = 1.44 from the 17 runs. The rms fluctuation of the 17 values of C about the mean is about 0.19. The accuracy of absolute level determination is reported as 10%. The mean value of C rises if best visual fits are made to curves like that in Fig. 10 instead of simply to straight lines.[19] This is because the curve approaches the asymptotic inertial-range line gradually. Heisenberg's transfer expression[3] gives a sharper knee. The mean value rises further if the longer runs are given greater weight, as Figs. 10 and 12 suggest.

Probably the following conclusions are justified: (1) The experimental data are consistent with Kolmogorov's theory. (2) The data suggest that the abridged LHDI prediction for C is better than an order-of-magnitude approximation to the correct value. (3) The abridged LHDI value appears to be high rather than low, but the data do not set a lower bound to the magnitude of the error nor determine its sign unequivocally. On the theoretical side, the approximations made in deriving the LHDI equations are sufficiently drastic that if theory and experiment agreed to better than the order of 10% it would be an accident. An interesting question is how much the abridged LHDI value of C differs from the prediction of the unabridged equations. Numerical integration of the latter in the inertial range appears to be feasible.

Figure 13 shows the computed values of $(k/k_s)^{5/3}\phi_{tot}(k)/(\varepsilon^{1/4}\nu^{5/4})$ plotted together with data obtained by M. M. Gibson[20] in a round air jet at $R_\lambda \sim 750$. The data were normalized by values of ε determined by Gibson

from the ϕ_1 values only. For the off-axis run, this ϵ agrees, to within the accuracy of determination, with the ϵ determined graphically from the ϕ_{tot} values. For the on-axis run, the ϕ_{tot} values give a larger ϵ, but they yield so irregular a dissipation spectrum that accurate determination is impossible. Therefore the on-axis points for ϕ_{tot} should be displaced downward, along lines of slope -4/3, by an uncertain amount.[19]

Gibson estimates C = 1.57 for the on-axis run and C = 1.62 for the off-axis run, on the basis of visual straight-line fits to the ϕ_1 measurements only. As in the sea-water experiments, these values rise if fits are made to scaled theoretical curves instead. Both runs exhibit anisotropy in the inertial range. For this reason, and because ϕ_1 represents only 3/11 of the energy in an isotropic -5/3 range, it seems more justified to compare ϕ_{tot} with isotropic theory, rather than ϕ_1. But the argument loses force if the transverse spectrum measurements are less reliable than the longitudinal.

It should be stressed in conclusion that no reported experiments confirm the $k^{-5/3}$ asymptotic spectrum law beyond reasonable doubt. Actually, the data at $k/k_s < .01$ on Figs. 10 and 12 fit, say, $k^{-7/4}$ better than $k^{-5/3}$, but the scatter is so great that no inconsistency with $k^{-5/3}$ can be inferred. Clearly an inertial range of many decades extent is needed for a definitive answer. Corrections of logarithmic type to the $k^{-5/3}$ law would be particularly difficult to resolve.

APPENDIX. NUMERICAL METHODS

The numerical integrations are based on a scheme described in detail previously.[9] The wavenumber integrations in (2.6)-(2.8) are performed just as in Ref. 9. For decay studies, (2.6)-(2.8) are integrated forward in time from t_0 by a modification of the time-integration scheme of Ref. 9: The first two terms on the right-hand sides of (2.7) and (2.8) are treated in parallel with the νk^2 terms on the left-hand sides. Thus, for (2.7), a function $N(k;t|r)$ is defined by

$$N(k;t|r)U(k;t|r) = \iint_\Delta [C_{kpq}U(k;t|r) - D_{kpq}U(p;t|r)] \int_r^t U(q;t|s)ds, \qquad (A1)$$

and the contribution of the two terms is included by replacing νk^2 with $\nu k^2 + N(k;t|r)$ in the scheme of Ref. 9. $N(k;t|r)$ is evaluated at the mid-point of each time step, like the other quantities in the scheme. The analogous procedure is used for (2.8). This modification gives improved stability and accuracy. The C and D terms on the right-hand side of (A1) are treated in strict parallel with each other to avoid errors from the effect of time and wavenumber discretizing upon the cancellations of the small-q contributions.

For the steady-state solution of (5.4) and (5.5), this method is augmented by an iteration procedure. The time limit ∞ in (5.5) is truncated to a large finite value $M\Delta t$ (M integer). Initial guesses $\overline{G}^0(\tau)$ and $\overline{R}^0(\tau)$ are taken (identical Gaussian functions). The values $\overline{G}(0) = 1$, $\overline{R}(0) = 1$ are held fixed and improved functions obtained by a modification of the scheme

$$\bar{G}^r(\tau_n) = \frac{1}{2}\{\bar{G}^{r-1}(\tau_n) + \bar{G}^r(\tau_{n-1}) + \frac{1}{2}\Delta t[\bar{H}(\tau_n) + \bar{H}(\tau_{n-1})]\},\ \bar{H}(0) = 0,$$

$$\bar{R}^r(\tau_n) = \frac{1}{2}\{\bar{R}^{r-1}(\tau_n) + \bar{R}^r(\tau_{n-1}) + \frac{1}{2}\Delta t[\bar{S}(\tau_n) + \bar{S}(\tau_{n-1})]\},\ \bar{S}(0)=0. \quad (A2)$$

Here $\bar{G}^r(\tau_n)$, $\bar{R}^r(\tau_n)$ is the rth approximation at the nth time step, and $\bar{H}(\tau)$, $\bar{S}(\tau)$ are the right-hand sides of (5.4), (5.5). For each r, (A2) is used for each n in succession, starting with n = 1 [$\tau_n = n\Delta t$ (n = 1,2, ...M)]. At each time-step, $\bar{S}$ and $\bar{H}$ are evaluated by the trapezoidal rule of Ref. 9, using always the best available values of $\bar{G}$ and $\bar{R}$: As soon as $\bar{G}^r(\tau_n)$ and $\bar{R}^r(\tau_n)$ are computed for any r and n, the old values $\bar{G}^{r-1}(\tau_n)$ and $\bar{R}^{r-1}(\tau_n)$ are discarded completely. Functions like $\bar{R}(w^{2/3}s)$ are evaluated from the $\bar{R}(\tau_n)$ by two-point interpolation. The modification of (A2), in accord with (A1) seq., is to replace $\frac{1}{2}[\bar{S}(\tau_n) + \bar{S}(\tau_{n-1})]$ as follows:

$$\frac{1}{2}\Delta t[\bar{S}(\tau_n) + \bar{S}(\tau_{n-1})] \to \left[\frac{1 - \exp\{-\frac{1}{2}[\bar{N}(\tau_n) + \bar{N}(\tau_{n-1})]\Delta t\}}{\bar{N}(\tau_n) + \bar{N}(\tau_{n-1})}\right]$$

$$\times [\bar{S}(\tau_n) + \bar{S}(\tau_{n-1})], \quad (A3)$$

where $-\bar{N}(\tau)\bar{R}(\tau)$ is defined as the first two terms on the right-hand side of (5.5). The $\bar{G}$ equation is treated in parallel fashion.

The iteration scheme was found to converge reliably but slowly; e.g., $|\bar{R}^r(\tau_n) - \bar{R}^{r-1}(\tau_n)|$ decreased typically by 20% per iteration. Convergence is markedly speeded by repeated cycles of iteration-followed-by-extrapolation. The extrapolation assumes geometrically decreasing errors (the errors do decrease nearly geometricallly).

Equation (5.11) is integrated by the same wavenumber discretizing used in (5.4) and (5.5). The contributions from wavenumber triads with different α values are accumulated separately so as to yield $W(\alpha)$ without the need for further calculation.

The numerical values reported in the text come from a calculation in which the v and w integrations in (5.4), (5.5) extend over the range $2^{-145/12}$ ($\sim 2.3 \times 10^{-4}$) to $2^{79/12}$ ($\sim 96.$), which is divided into 112 one-sixth-octave steps according to the method of Ref. 9. The contributions of higher w and v values are approximated by correction terms based on (4.13); these corrections are quite small. The s integrations are truncated at $s = 20$, and $\overline{R}(\tau)$, $\overline{G}(\tau)$ are computed over $(0 < \tau \leq 20)$ at steps of 0.1. Iteration was continued until the change in C per iteration was <0.1%, with extrapolation indicating residual error <0.3%. Changes of $\overline{R}(s)$ and $\overline{G}(s)$ per iteration were less than both .001 and 1%, with extrapolation indicating residual errors less than .005 and 5%. Errors from finite step-sizes and truncation were estimated by varying the relevant parameters and extrapolating. The estimated total error in C from all causes is about 1%. Errors in some of the other dimensionless constants are larger, but are not expected to exceed 3%. The theory probably does not justify more accurate computation.

Six to eight decimal digits were carried in the computations, and all final numbers reported in the text are rounded to two or three digits. To six digits, the values found for (6.1) and (6.2) are $C = 1.76612$, $I_G = 1.04404$, $I_R = 1.87438$, $I_1 = .760973$, $I_2 = -.188401$. The values computed for the left and right sides of (8.26) are 8.73360 and 8.96029, which agree to within 2.6%.

For rough calculations, the computed functions $G(\tau)$ and $R(\tau)$ are adequately approximated by

$$G(\tau) = 4\exp(2\tau/I_G)/[1+\exp(2\tau/I_G)]^2, \quad R(\tau) = [1+(\tfrac{1}{2}\pi\tau/I_R)^2]^{-1}. \quad (A4)$$

The decay calculation used in Sec. 9 was performed by taking $\nu = .008$, $E(k,t_0) = 6.29\,k^{-5/3}$, and a k range $2^{-19/6}$ ($\sim .11$) to $2^{37/6}$ ($\sim 72.$) discretized into 28 one-third octave steps. Equations (2.6)-(2.8) were integrated, with the techniques described above, for 20 time steps $\Delta t = .02$, by which time changes in the normalized energy and dissipation spectra were imperceptible on automatically generated plots. Final values $k_s = 58.5$ and $R_\lambda = 440$ were obtained, with respective changes of 0.1% and 0.2% per time step. The estimated overall computational errors are not significant for the comparison with experiment in Figs. 10-13, provided $k/k_s < 0.6$. The difference between this $R_\lambda = 440$ spectrum and an $R_\lambda = \infty$ spectrum normalized in the same way probably is negligible also. It was to minimize the difference that the initial spectrum was taken $\propto k^{-5/3}$ down to the lowest wavenumber retained.

All the calculations were performed on the IBM 7094 computer at the Goddard Institute for Space Studies. The plots were generated on a General Dynamics S-C 4020 Recorder.

REFERENCES

1. R. H. Kraichnan, Phys. Fluids 8, 575 (1965); errata, 9, xxx (1966). The errata are appended to this reference list.

2. The terms containing C_{kpq} appear in Ref. 1 with the p integrations performed. The present form is better for numerical work (see Appendix).

3. W. Heisenberg, Z. Phys. 124, 628 (1948).

4. A. A. Townsend, Proc. Roy. Soc. London A208, 534 (1951).

5. G. K. Batchelor, I. D. Howells, and A. A. Townsend, J. Fluid Mech. 5, 134 (1959).

6. H. Lamb, Hydrodynamics (Cambridge University Press, 1932), sixth edition.

7. R. H. Kraichnan, Phys. Fluids 7, 142 (1964).

8. Cf. Ref. 3, Eqs. (85)-(91).

9. R. H. Kraichnan, Phys. Fluids 7, 1030 (1964); erratum 8, 210 (1965).

10. Incorrect computations of inertial-range parameters are reported by R. H. Kraichnan, Phys. Fluids 8, 995 (1965). See errata, 9, xxx (1966). The errata are appended to this reference list.

11. J. L. Lumley, in Mécanique de la Turbulence (Centre National de la Recherche Scientifique, Paris, 1962).

12. G. K. Batchelor, Theory of Homogeneous Turbulence (Cambridge University Press, 1953).

13. C. C. Lin, Proc. Nat. Acad. Sciences 46, 1147 (1960).

14. E. Inoue, J. Met. Soc. Japan 28, 441 (1950).

15. A. M. Oboukhov, Advances in Geophysics 6, 113 (1959).

16. C. C. Lin, Proc. Nat. Acad. Sciences 46, 566 (1960), Eq. (3). Lin's τ is the negative of that in (8.12).

17. A. M. Oboukhov, Dokl. Akad. Nauk S.S.S.R. 66, 17 (1949). See also Ref. 12, Chapter 8.

18. H. L. Grant, R. W. Stewart, and A. Moilliet, J. Fluid Mech. 12, 241 (1962). The data in Figs. 10-12 are machine-plotted from tabulations of corrected and normalized spectra kindly supplied by Dr. Grant in November 1964. The corrections are for errors in ν, which affect Fig. 14 of this reference but are corrected elsewhere throughout the published paper.

19. The transformation $\phi_1'(k) = \alpha^{9/4}\phi_1(\alpha^{3/4}k)$ leaves ϵ and k_s unchanged and changes the Kolmogorov constant according to $C' = \alpha C$. Thus, a family of curves with different values of C' is obtained by translating the curve of Fig. 10 along a line with slope -4/3 on the log-log plot. This makes the mechanics of graphical fitting quite simple. Conversely, a change $\epsilon' = \beta\epsilon$ in the experimental value of ϵ shifts the plotted experimental points along lines of slope -4/3 by an amount determined by $C' = \beta^{-2/3}C$.

20. M. M. Gibson, J. Fluid Mech. 15, 161 (1963). The data in Fig. 13 are machine-plotted from tabulations kindly supplied by Dr. Gibson in October 1963. (The values of ν given in the published paper are ten times too small.)

ERRATA: LAGRANGIAN-HISTORY CLOSURE APPROXIMATION FOR TURBULENCE

[Phys. Fluids 8, 575 (1965)]

Robert H. Kraichnan

Peterborough, New Hampshire

The minus signs should be changed to plus signs in the third line of (8.10), the first line of (8.11), and the second, fifth, and seventh lines of (8.12). In the sixth line of (8.11), p_c should be q_c. In the fourth line of (10.9), the plus sign should be a minus sign.

ERRATA: PRELIMINARY CALCULATION OF THE KOLMOGOROV TURBULENCE SPECTRUM

[Phys. Fluids 8, 995 (1965)]

Robert H. Kraichnan

Peterborough, New Hampshire

In the third line of (3), the plus sign should be a minus sign. This error was carried through the numerical computations. The corrected numerical coefficients in (10) are 1.60, 0.50, 0.99, in order of appearance. The corrected coefficients in (10') are 1.77, 0.53, 0.96. Corrections in the Figures are small. For corrected Figures, see R. H. Kraichnan, Phys. Fluids 9, xxx (1966) [Research Report 8].

FIGURE CAPTIONS

Fig. 1. Integration paths for following the evolution of the Lagrangian velocity.

Fig. 2. The inertial-range Lagrangian time-correlation and response functions $R(\tau)$ and $G(\tau)$, versus nondimensional time difference τ.

Fig. 3. Dimensionless measures of localness of inertial-range energy transfer, versus maximum to minimum wavenumber ratio α. Here $\overline{W}(\alpha) = W(\alpha)/\varepsilon$ and $\overline{P}(\alpha) = P(\alpha)/\varepsilon$.

Fig. 4. Dimensionless Lagrangian spacetime, or two-particle, structure functions $F(s)$ and $F_{\parallel}(s)$ in the inertial range, versus dimensionless time difference s. The straight line is the function κs of (7.12a).

Fig. 5. Dimensionless Eulerian spacetime structure functions $F^{E}(s)$ and $F_{\parallel}^{E}(s)$ in the inertial range, versus dimensionless time difference s.

Fig. 6. Nondimensional measures $\dot{F}(s)$ and $\dot{F}_{\parallel}(s)$ of the inertial-range covariance of one particle's velocity with a second particle's prior acceleration, versus dimensionless time difference s.

Fig. 7. Nondimensional time-displaced, inertial-range cospectrum $Q(s)$ of pressure gradient and prior Lagrangian velocity, versus nondimensional time difference s.

Fig. 8. Nondimensional inertial-range covariances $Z(s)$ and $Z_{x}(s)$ of one particle's prior velocity with a second particle's acceleration, versus dimensionless time difference s.

Fig. 9. Nondimensional inertial-range, two-particle, Lagrangian acceleration covariances $\dot{Z}(s)$ and $\dot{Z}_{x}(s)$, versus dimensionless time difference s.

Fig. 10. Computed nondimensionalized spectrum function $k^{5/3}\phi_1(k)$ in the inertial and dissipation ranges compared with the October 1959 data of Grant, Stewart, and Moilliet. Circles, run 0905/3/10/59; dots, 0907/3/10/59; plus signs, 0915/3/10/59. (The low-wavenumber terminus of the decay curve lies within the fourth circle from the left.)

Fig. 11. Computed nondimensionalized dissipation spectrum $k^2\phi_1(k)$ compared with the October data of Grant, Stewart, and Moilliet. Circles, run 0905/3/10/59; dots, 0907/3/10/59; plus signs, 0915/3/10/59.

Fig. 12(a). Computed function $k^{5/3}\phi_1(k)$ compared with the three longest runs obtained by Grant, Stewart, and Moilliet on 1 February 1960. Circles, run 1126/1/2/60; dots, 1203/1/2/60; plus signs, 1331/1/2/60.

Fig. 12(b). Computed function $k^{5/3}\phi_1(k)$ compared with the three longest runs obtained by Grant, Stewart, and Moilliet on 2 February 1960. Circles, run 1301/2/2/60; dots, 1316/2/2/60; plus signs, 1445/2/2/60.

Fig. 13. Comparison of computed spectra with data of M. M. Gibson. Upper curve and data: computed function $k^{5/3}\phi_{tot}(k)$; dots, on-axis run; plus signs, off-axis run. Lower curve and data: computed function $k^{5/3}\phi_1(k)$; dots, on-axis run; plus signs, off-axis run. The data for ϕ_{tot} appear only at those wavenumbers where Gibson obtained the necessary measurements of both longitudinal and transverse spectra.

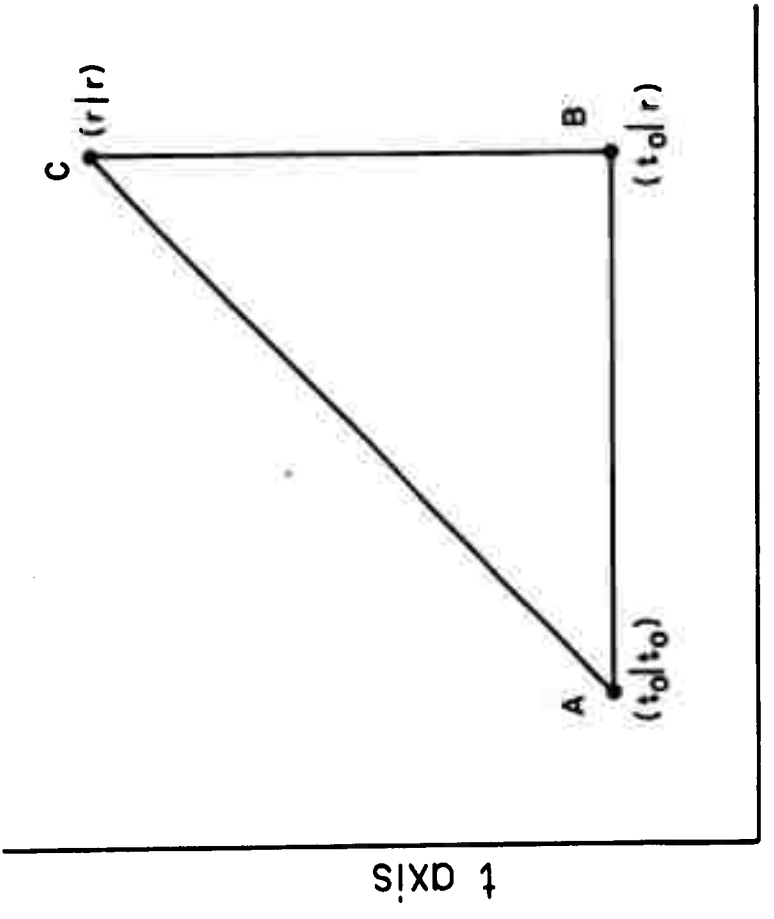

FIGURE 1

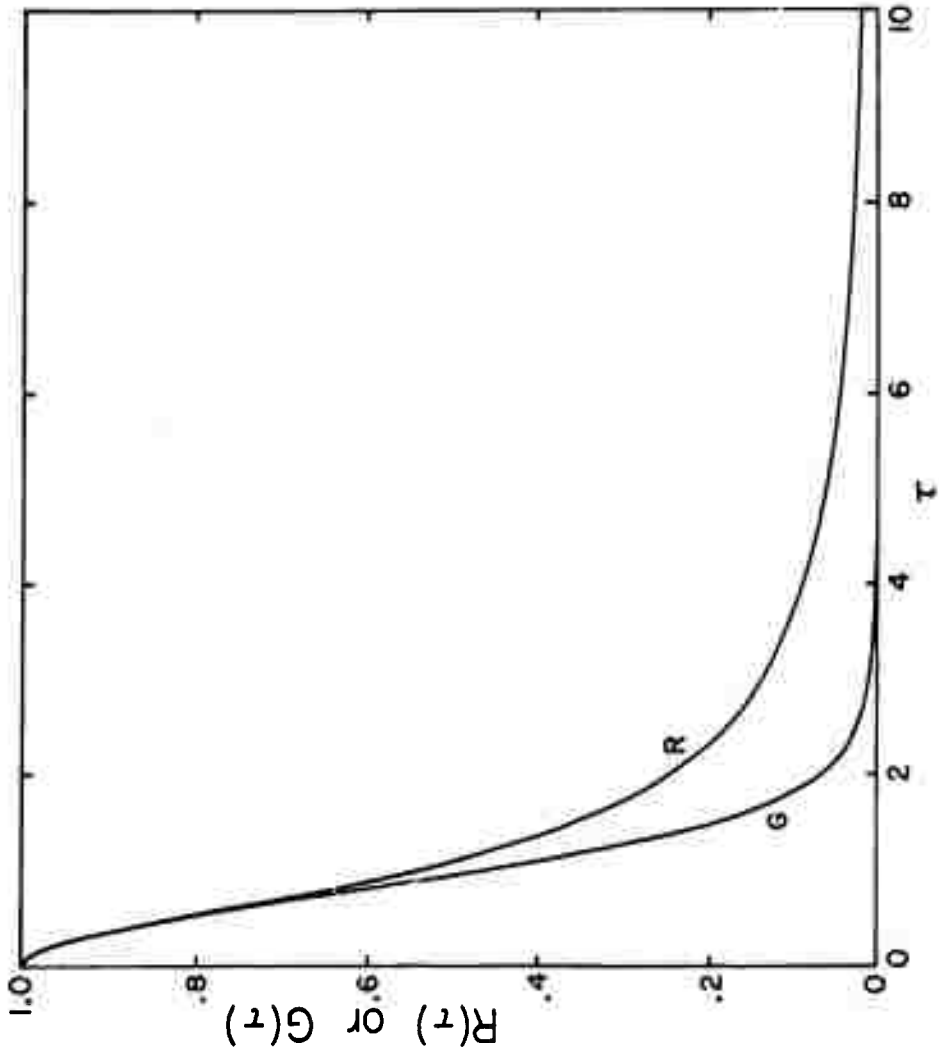

FIGURE 2

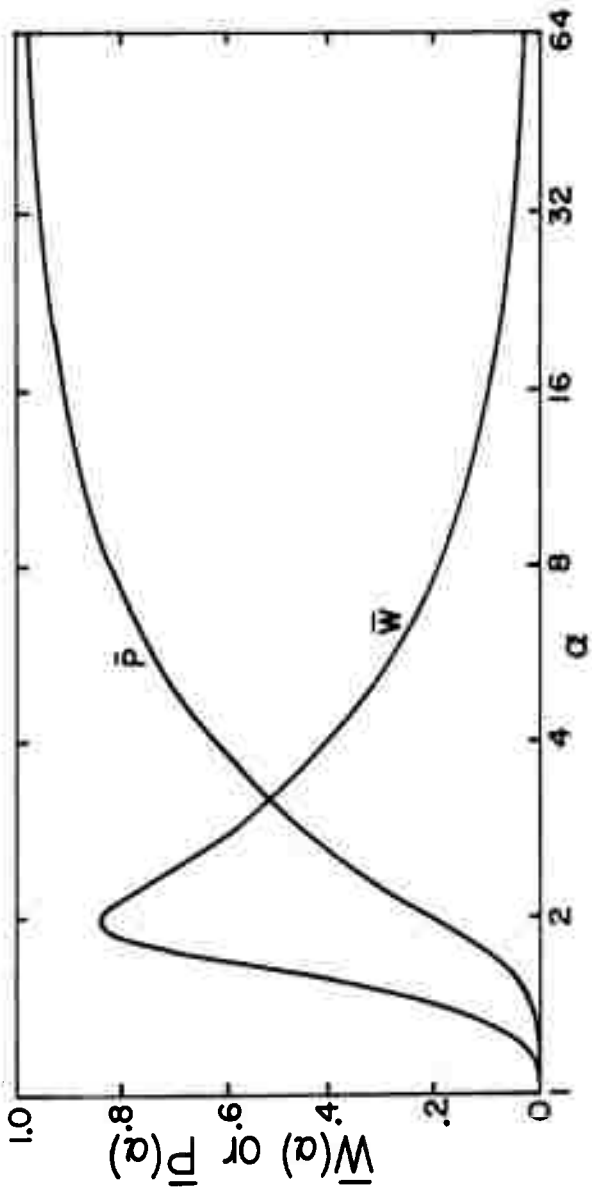
$\overline{W}(\alpha)$ or $\overline{P}(\alpha)$
1.0
.8
.6
.4
.2
0
1
2
4
8
16
32
64
α
$\overline{P}$
$\overline{W}$

FIGURE 3

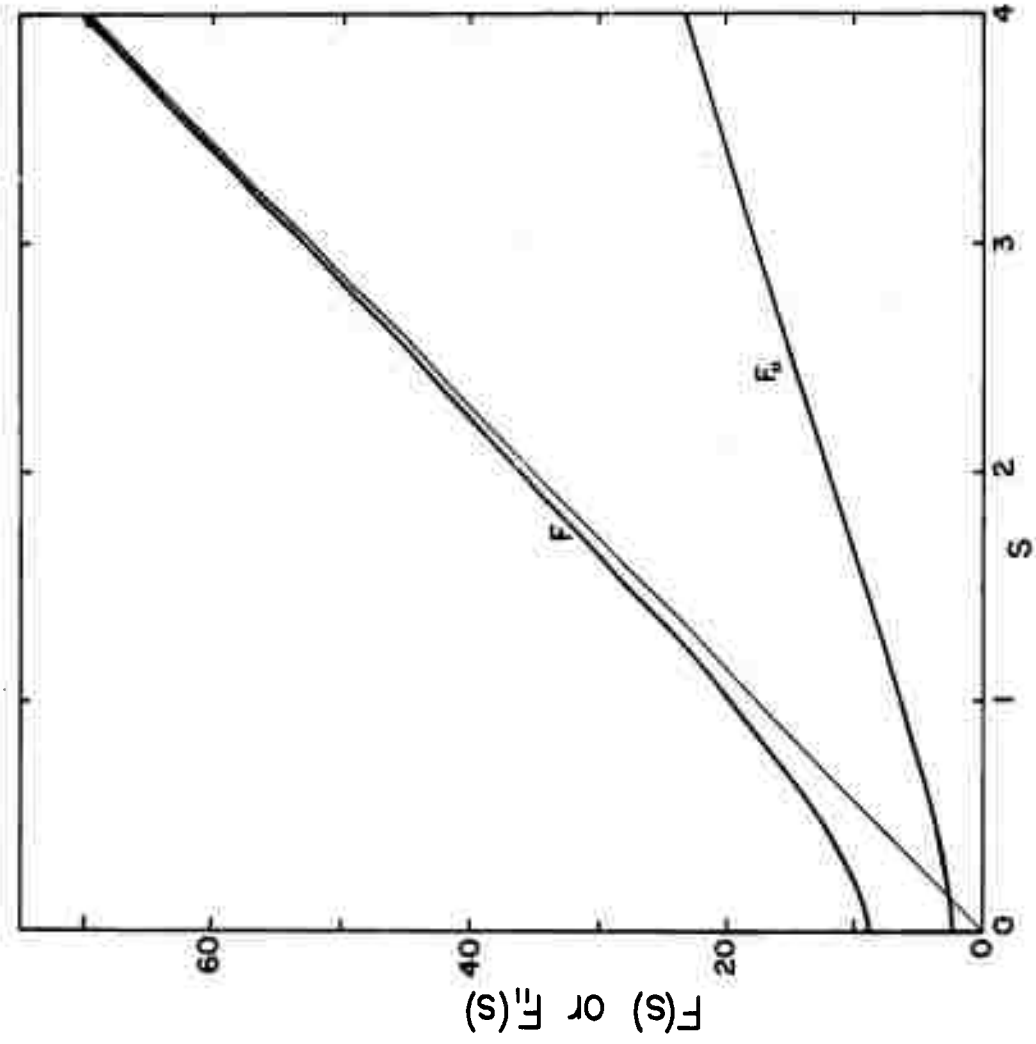

FIGURE 4

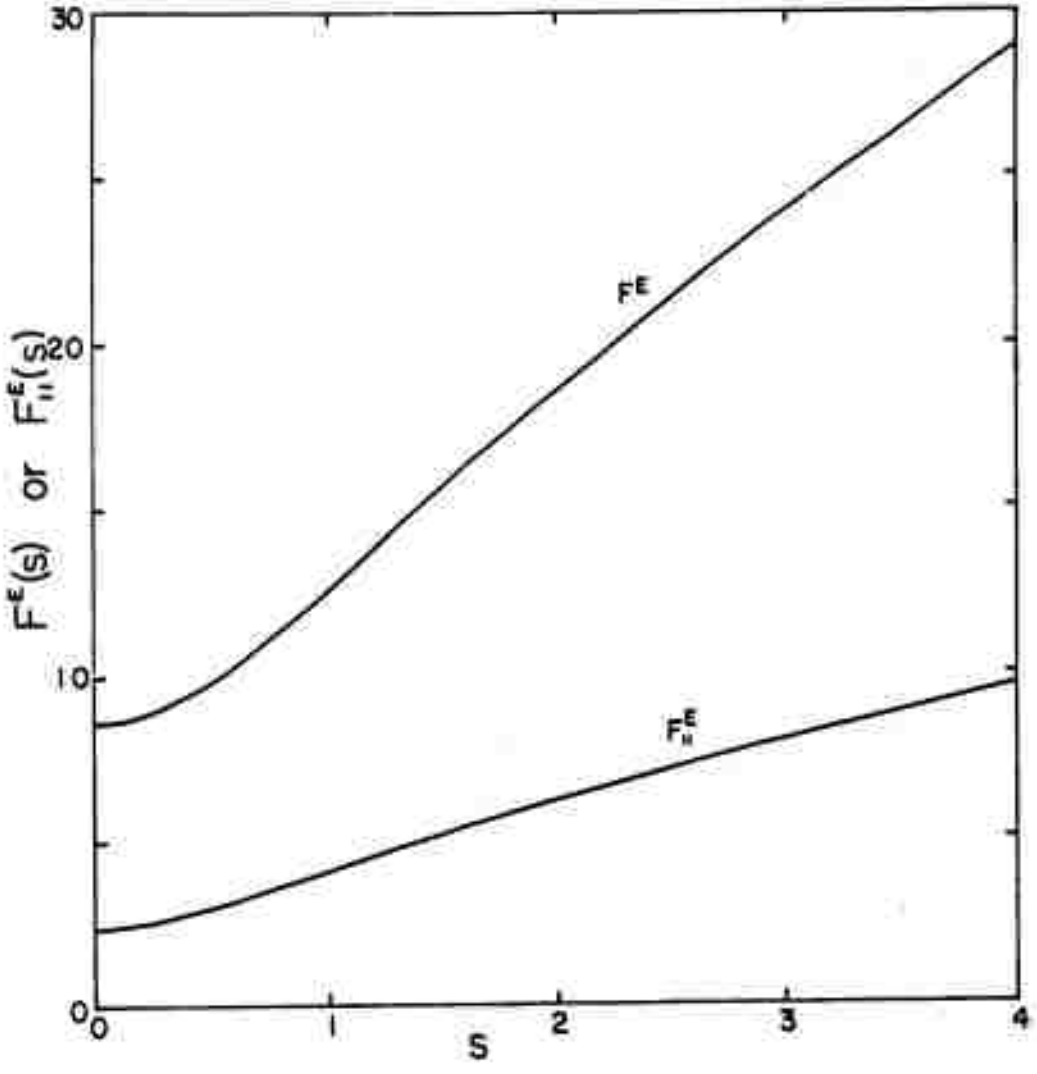

FIGURE 5

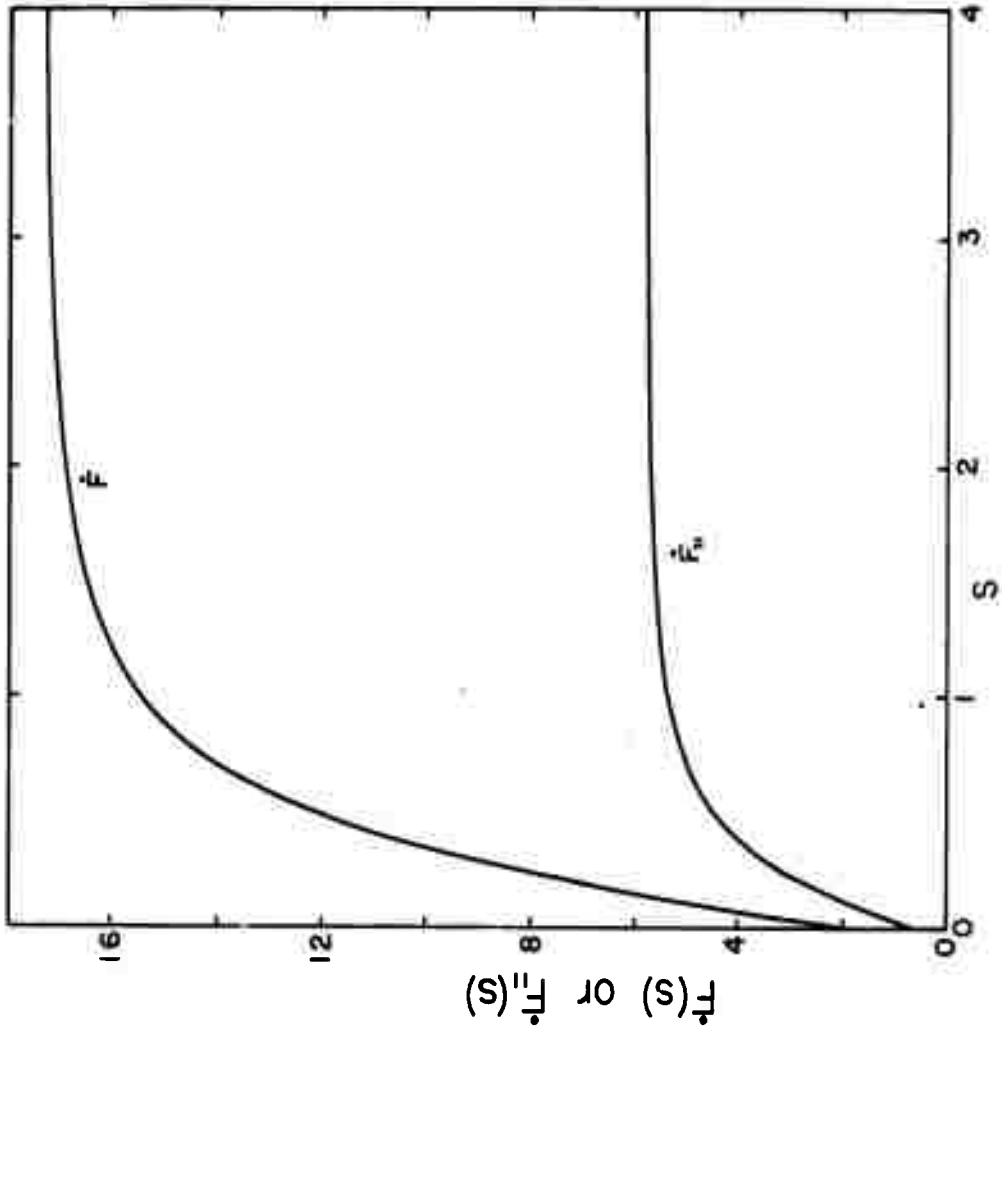

FIGURE 6

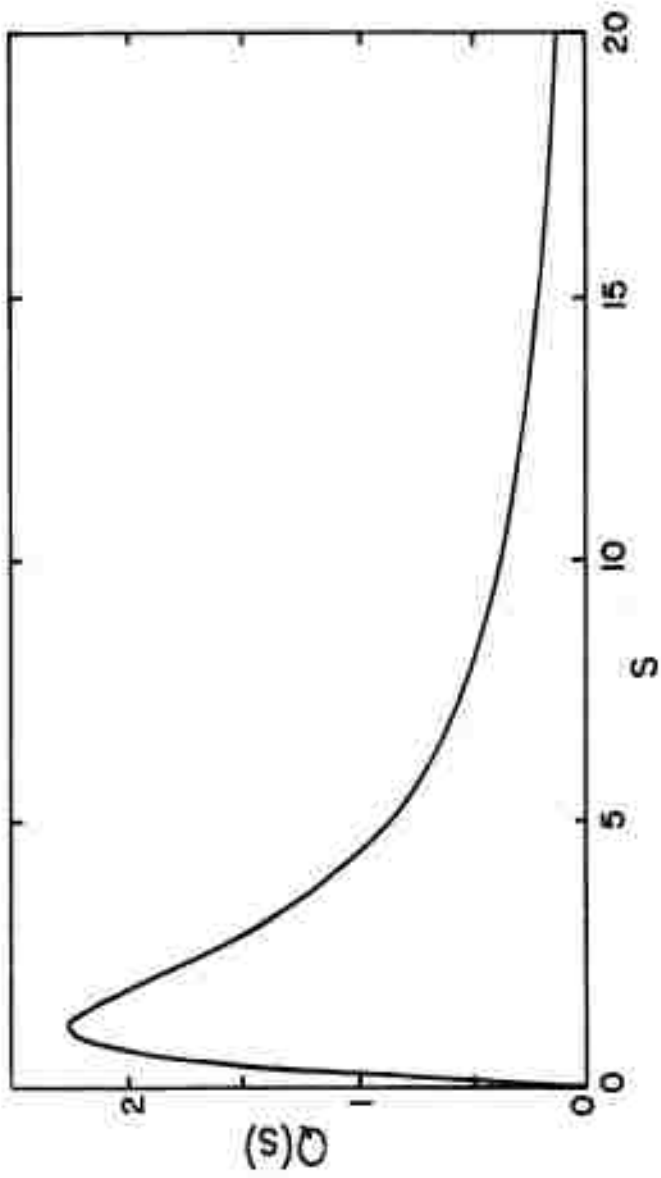

FIGURE 7

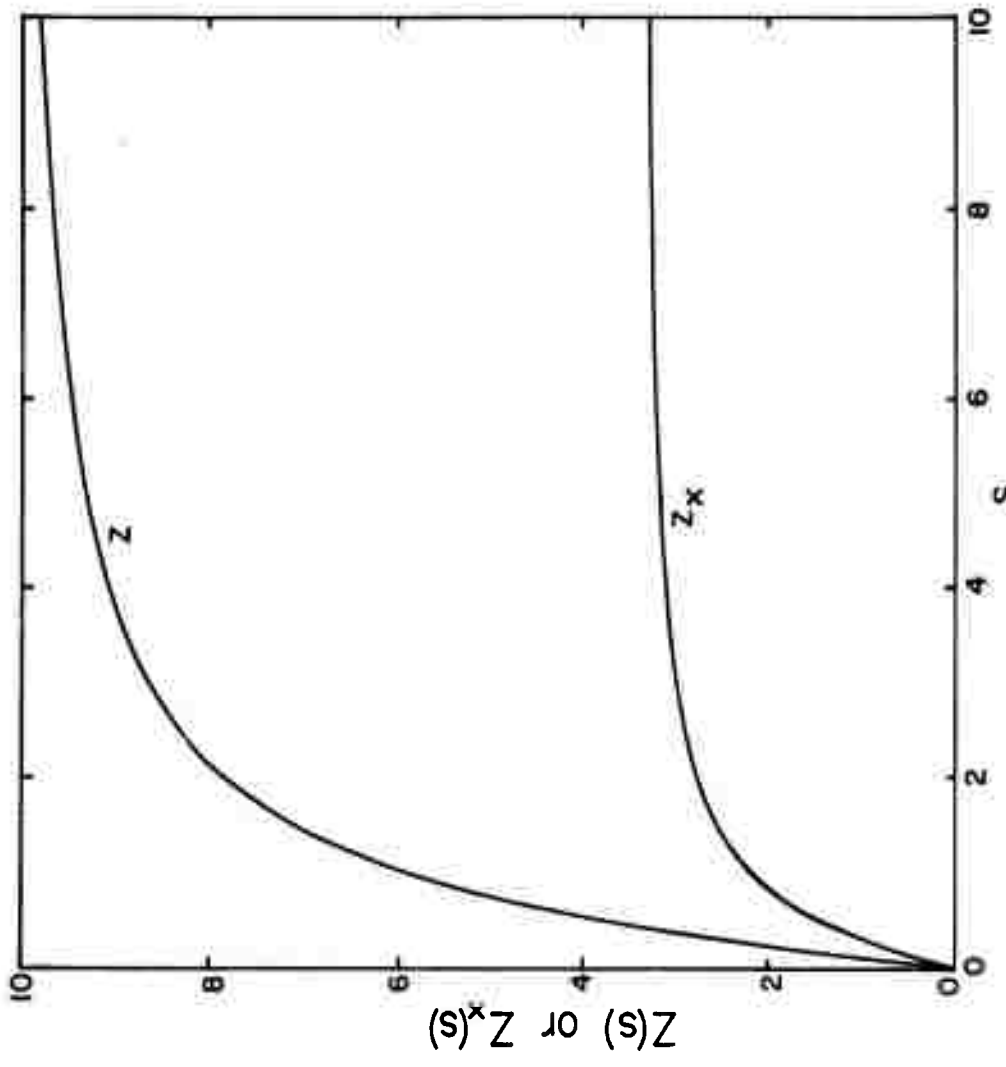

FIGURE 8

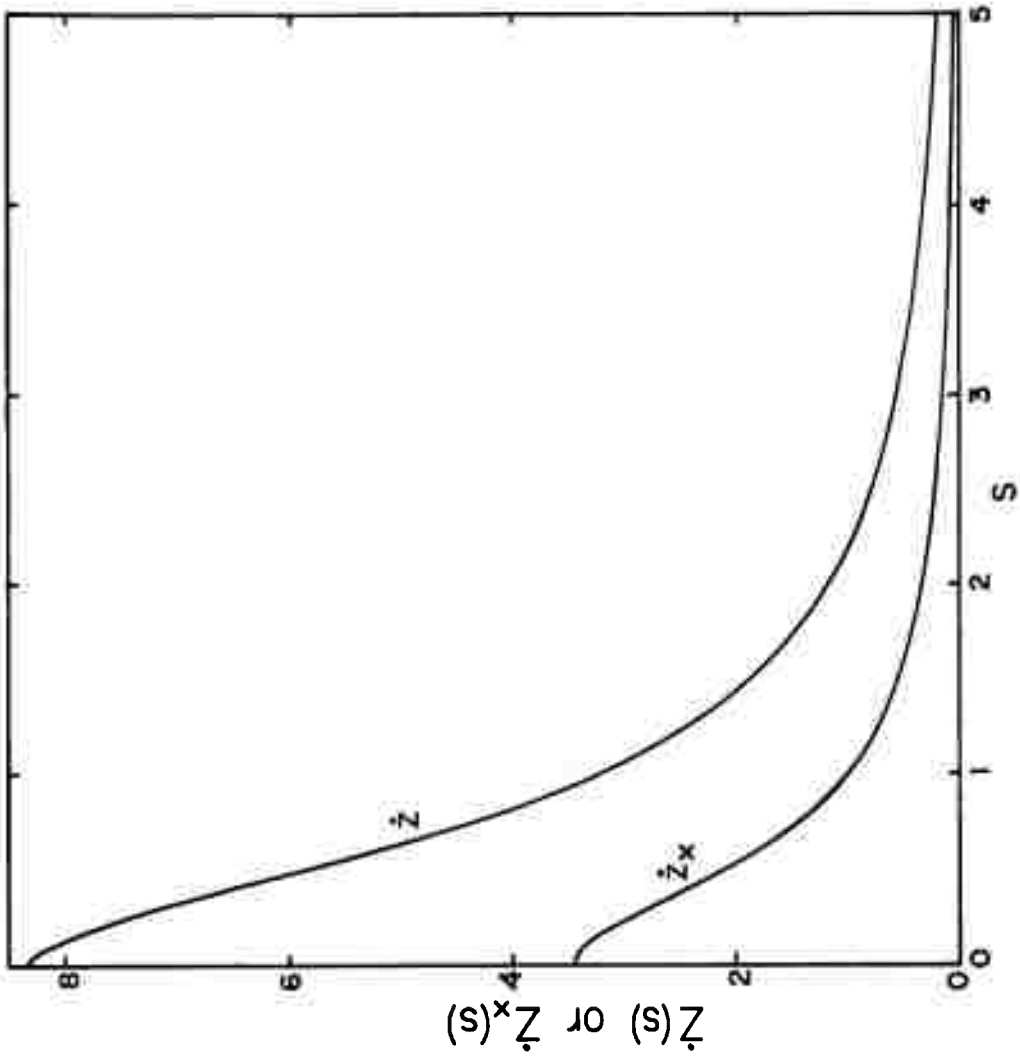

FIGURE 9

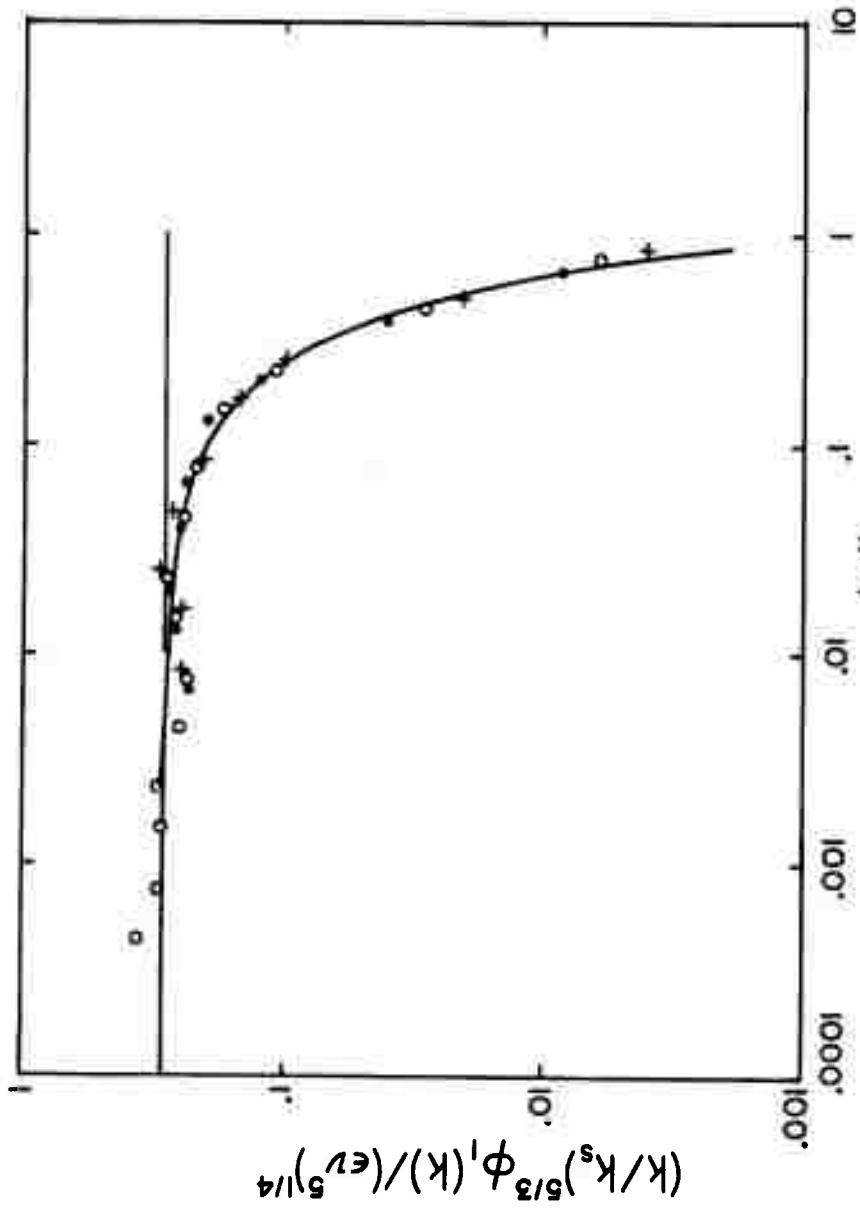
$(k/k_s)^{5/3}\Phi_1(k)/(\epsilon\nu^5)^{1/4}$
100.
10.
1.
.1000
.0100
.0010
.0001
.01
.1
1
10
k/k_s

FIGURE 10

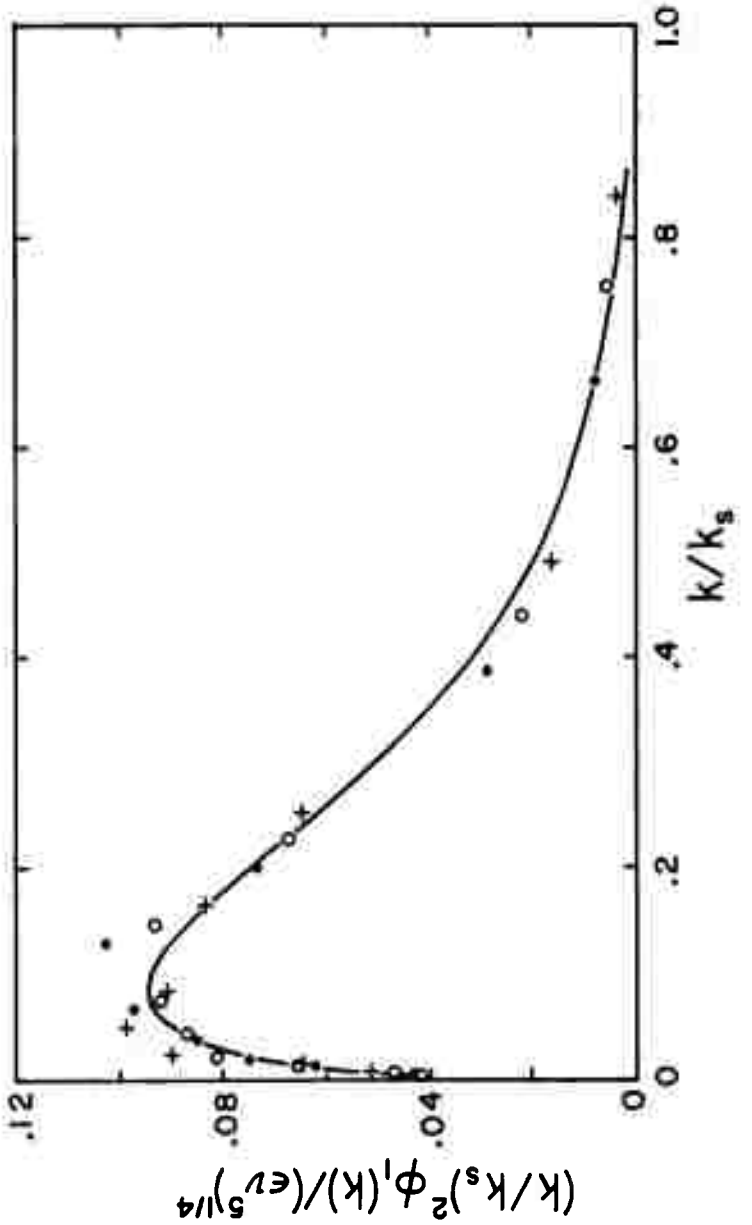

FIGURE 11

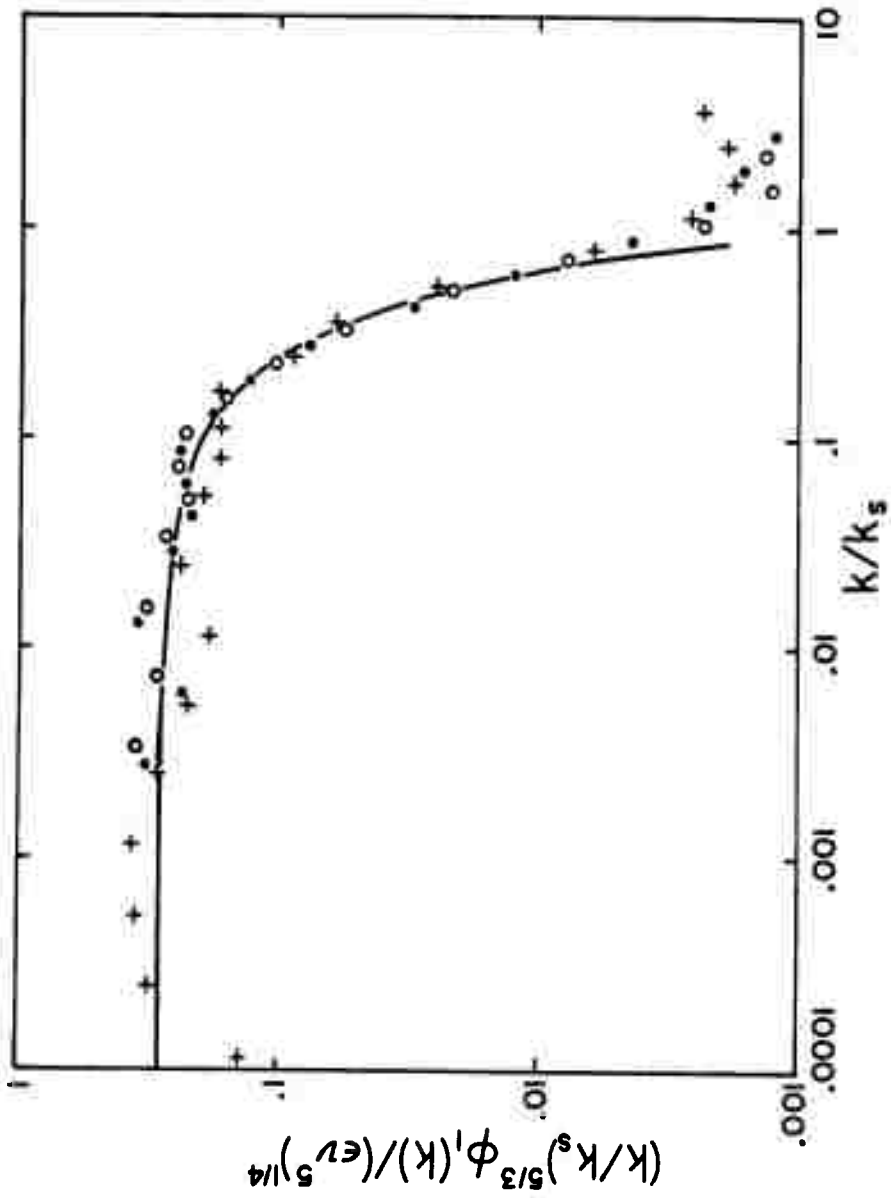
$(k/k_s)^{5/3}\Phi_l(k)/(\epsilon\nu^5)^{1/4}$
100.
10.
1.
.1
.01
.001
.0001
10
1
.1
.01
.001
k/k_s

FIGURE 12(a)

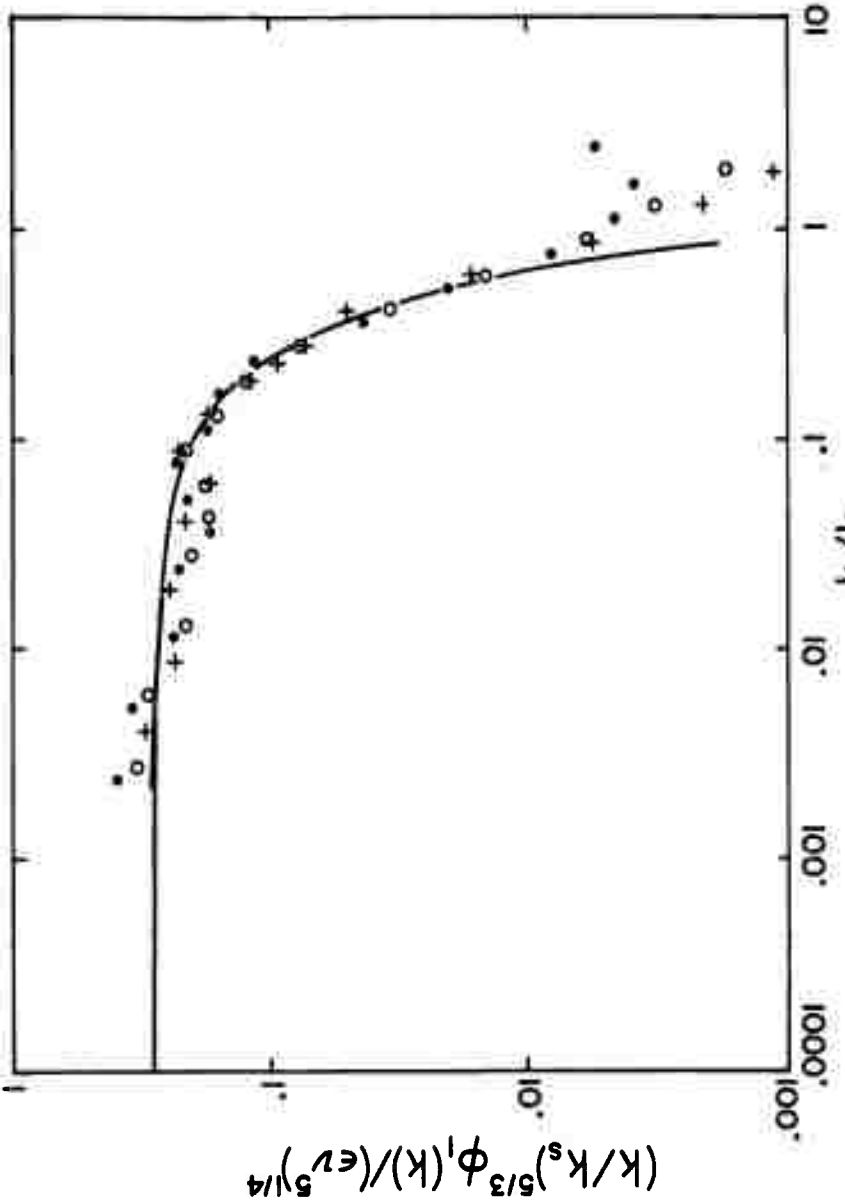

FIGURE 12(b)

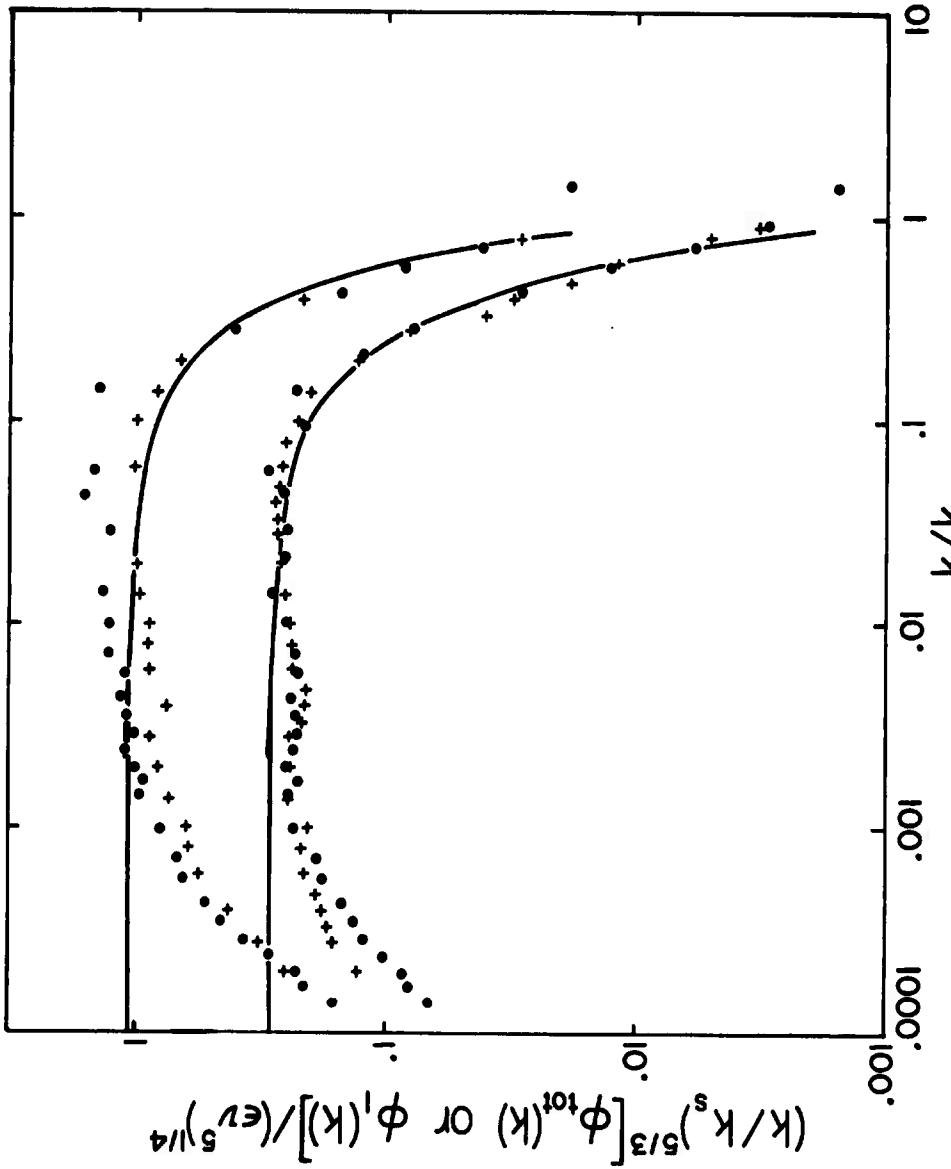
$(k/k_s)^{5/3}[\phi_{tot}(k)$ or $\phi_i(k)]/(\epsilon\nu^5)^{1/4}$
100.
10.
1.
.1
.01
.001
.0001
10
1
k/k_s

FIGURE 13

DOCUMENT CONTROL DATA - R&D

(Security classification of title, body of abstract and indexing annotation must be entered when the overall report is classified)

1. ORIGINATING ACTIVITY *(Corporate author)* ROBERT H. KRAICHNAN PETERBOROUGH, NEW HAMPSHIRE	2a. REPORT SECURITY CLASSIFICATION UNCLASSIFIED 2b GROUP

3. REPORT TITLE

ISOTROPIC TURBULENCE AND INERTIAL-RANGE STRUCTURE IN THE ABRIDGED LHDI APPROXIMATION

4. DESCRIPTIVE NOTES *(Type of report and inclusive dates)*

5. AUTHOR(S) *(Last name, first name, initial)*

ROBERT H. KRAICHNAN

6. REPORT DATE	7a. TOTAL NO. OF PAGES	7b. NO. OF REFS
JANUARY 1966	84 + ii	20

8a. CONTRACT OR GRANT NO.	9a. ORIGINATOR'S REPORT NUMBER(S)
Nonr 4307(00) b. PROJECT NO. RR 009 01 01 c. Task NR 062-309 d.	RESEARCH REPORT NO. 8 9b. OTHER REPORT NO(S) *(Any other numbers that may be assigned this report)*

10. AVAILABILITY/LIMITATION NOTICES

DISTRIBUTION OF THIS REPORT IS UNLIMITED

11. SUPPLEMENTARY NOTES	12. SPONSORING MILITARY ACTIVITY
	FLUID DYNAMICS BRANCH, OFFICE OF NAVAL RESEARCH

13. ABSTRACT

The abridged LHDI (Lagrangian-History Direct Interaction) closure approximation is interpreted physically and used to analyze energy transfer, effective eddy viscosities, and Lagrangian spacetime statistics in stationary and decaying isotropic turbulence. The results are then specialized to the inertial range. Numerical values are predicted for the Kolmogorov constant, the asymptotic eddy viscosities due to inertial-range wavenumbers, and the dimensionless constant in Inoue's formula for the mean-square change of Lagrangian velocity with time. Computed curves are presented for the localness of energy transfer, for Lagrangian spacetime structure functions, and for Lagrangian spacetime acceleration-acceleration and velocity-acceleration covariances. Inertial-range Eulerian spacetime structure functions also are computed. The predicted absolute Kolmogorov spectrum in the inertial and dissipation ranges is compared with data of Grant, Stewart, and Moilliet, and of M. M. Gibson.

DD FORM 1 JAN 64 1473

14. KEY WORDS	LINK A		LINK B		LINK C	
	ROLE	WT	ROLE	WT	ROLE	WT
TURBULENCE						
ENERGY-TRANSFER						
LAGRANGIAN STATISTICS						
INERTIAL RANGE						
STRUCTURE FUNCTIONS						

INSTRUCTIONS

1. **ORIGINATING ACTIVITY:** Enter the name and address of the contractor, subcontractor, grantee, Department of Defense activity or other organization *(corporate author)* issuing the report.

2a. **REPORT SECURITY CLASSIFICATION:** Enter the overall security classification of the report. Indicate whether "Restricted Data" is included. Marking is to be in accordance with appropriate security regulations.

2b. **GROUP:** Automatic downgrading is specified in DoD Directive 5200.10 and Armed Forces Industrial Manual. Enter the group number. Also, when applicable, show that optional markings have been used for Group 3 and Group 4 as authorized.

3. **REPORT TITLE:** Enter the complete report title in all capital letters. Titles in all cases should be unclassified. If a meaningful title cannot be selected without classification, show title classification in all capitals in parenthesis immediately following the title.

4. **DESCRIPTIVE NOTES:** If appropriate, enter the type of report, e.g., interim, progress, summary, annual, or final. Give the inclusive dates when a specific reporting period is covered.

5. **AUTHOR(S):** Enter the name(s) of author(s) as shown on or in the report. Enter last name, first name, middle initial. If military, show rank and branch of service. The name of the principal author is an absolute minimum requirement.

6. **REPORT DATE:** Enter the date of the report as day, month, year; or month, year. If more than one date appears on the report, use date of publication.

7a. **TOTAL NUMBER OF PAGES:** The total page count should follow normal pagination procedures, i.e., enter the number of pages containing information.

7b. **NUMBER OF REFERENCES:** Enter the total number of references cited in the report.

8a. **CONTRACT OR GRANT NUMBER:** If appropriate, enter the applicable number of the contract or grant under which the report was written.

8b, 8c, & 8d. **PROJECT NUMBER:** Enter the appropriate military department identification, such as project number, subproject number, system numbers, task number, etc.

9a. **ORIGINATOR'S REPORT NUMBER(S):** Enter the official report number by which the document will be identified and controlled by the originating activity. This number must be unique to this report.

9b. **OTHER REPORT NUMBER(S):** If the report has been assigned any other report numbers *(either by the originator or by the sponsor)*, also enter this number(s).

10. **AVAILABILITY/LIMITATION NOTICES:** Enter any limitations on further dissemination of the report, other than those imposed by security classification, using standard statements such as:

(1) "Qualified requesters may obtain copies of this report from DDC."

(2) "Foreign announcement and dissemination of this report by DDC is not authorized."

(3) "U. S. Government agencies may obtain copies of this report directly from DDC. Other qualified DDC users shall request through _____."

(4) "U. S. military agencies may obtain copies of this report directly from DDC. Other qualified users shall request through _____."

(5) "All distribution of this report is controlled. Qualified DDC users shall request through _____."

If the report has been furnished to the Office of Technical Services, Department of Commerce, for sale to the public, indicate this fact and enter the price, if known.

11. **SUPPLEMENTARY NOTES:** Use for additional explanatory notes.

12. **SPONSORING MILITARY ACTIVITY:** Enter the name of the departmental project office or laboratory sponsoring *(paying for)* the research and development. Include address.

13. **ABSTRACT:** Enter an abstract giving a brief and factual summary of the document indicative of the report, even though it may also appear elsewhere in the body of the technical report. If additional space is required, a continuation sheet shall be attached.

It is highly desirable that the abstract of classified reports be unclassified. Each paragraph of the abstract shall end with an indication of the military security classification of the information in the paragraph, represented as *(TS), (S), (C), or (U)*.

There is no limitation on the length of the abstract. However, the suggested length is from 150 to 225 words.

14. **KEY WORDS:** Key words are technically meaningful terms or short phrases that characterize a report and may be used as index entries for cataloging the report. Key words must be selected so that no security classification is required. Identifiers, such as equipment model designation, trade name, military project code name, geographic location, may be used as key words but will be followed by an indication of technical context. The assignment of links, roles, and weights is optional.